Article

Geochemical and Mineralogical Characterisation of Historic Zn–Pb Mine Waste, Plombières, East Belgium

Srećko Bevandić [1,*], Rosie Blannin [2], Jacqueline Vander Auwera [3], Nicolas Delmelle [3], David Caterina [4], Frederic Nguyen [4] and Philippe Muchez [1]

[1] Department of Earth and Environmental Sciences, KU Leuven, B-3001 Leuven, Belgium; philippe.muchez@kuleuven.be

[2] Helmholtz Institute Freiberg for Resource Technology, Helmholtz-Zentrum Dresden-Rossendorf, 09599 Freiberg, Germany; blanni70@hzdr.de

[3] Department of Geology, University of Liège, Quartier AGORA, B-4000 Liège, Belgium; jvdauwera@uliege.be (J.V.A.); nicolas.delmelle@uliege.be (N.D.)

[4] Urban and Environmental Engineering, University of Liège, B-4000 Liège, Belgium; David.Caterina@uliege.be (D.C.); F.Nguyen@uliege.be (F.N.)

* Correspondence: sreko.bevandi@kuleuven.be; Tel.: +32-16-19-42-16

Abstract: Mine wastes and tailings derived from historical processing may contain significant contents of valuable metals due to processing being less efficient in the past. The Plombières tailings pond in eastern Belgium was selected as a case study to determine mineralogical and geochemical characteristics of the different mine waste materials found at the site. Four types of material were classified: soil, metallurgical waste, brown tailings and yellow tailings. The distribution of the mine wastes was investigated with drill holes, pit-holes and geophysical methods. Samples of the materials were assessed with grain size analysis, and mineralogical and geochemical techniques. The mine wastes dominantly consist of SiO_2, Al_2O_3 and Fe_2O_3. The cover material, comprising soil and metallurgical waste is highly heterogeneous in terms of mineralogy, geochemistry and grain size. The metallurgical waste has a high concentration of metals (Zn: 0.1 to 24 wt.% and Pb: 0.1 to 10.1 wt.%). In the tailings materials, Pb and Zn vary from 10 ppm to 8.5 wt.% and from 51 ppm to 4 wt.%, respectively. The mining wastes comprises mainly quartz, amorphous phases and phyllosilicates, with minor contents of Fe-oxide and Pb- and Zn-bearing minerals. Based on the mineralogical and geochemical properties, the different potential applications of the four waste material types were determined. Additionally, the theoretical economic potential of Pb and Zn in the mine wastes was estimated.

Keywords: critical raw materials; geophysics; Mississippi Valley-type (MVT) deposits; Plombières; secondary resources; slags; tailings

1. Introduction

The demand for raw and critical raw materials (CRM) is growing day by day. This results in an increasing dependence of the world on a few countries, such as China, South Africa, USA and Russia, which are rich in CRM resources. Europe, in general, is highly dependent on the resources of foreign countries. Therefore, countries of the European Union are vulnerable to disruptions in CRM supply [1]. In the search for alternative sources of base metals and CRMs, some of the most promising resources are mine wastes, particularly tailings.

Tailings are fine-grained products from mineral processing (e.g., crushing, milling, flotation, etc.), which at the time of mining were categorized as waste. The properties of the tailings (e.g., mineralogy, grain size, chemistry) strongly depend on both the origin and treatment of the ore, as well as post-depositional processes [2]. Historic tailings may

contain significant concentrations of valuable metals, such as important base (e.g., Pb, Zn, Cu) and critical (e.g., In, Ge, Ga) metals, of which the latter were not previously economically feasible to recover. Therefore, the investigation of historic tailings is vital for determining the potential for economic exploitation of the remaining metals of interest [3–5]. Not only this, but the often-high heavy metal content of tailings combined with the propensity for sulphidic-rich tailings materials to produce acid mine drainage (AMD) means that tailings could also pose a significant risk to the environment [6,7]. Furthermore, mine wastes represent a potential risk for humans, as the contained metals and metalloids (e.g., Pb, Cr, Cd, As) can enter the human body via inhalation, digestion or even direct contact, to contribute towards a range of illnesses [8,9].

Individual mine waste dumps can reach up to 100,000 m³ [10]. However, there are often multiple mine waste or tailings dumps of the same or similar material at a single historical mine site. Historical mining regions have the potential for economic recoverability of metals and re-use of material and often show high risk to the environment [8]. When combining these vast quantities of mine wastes with the potential for both economic recovery of metals and environmental pollution, it is of great importance to investigate historic tailings, particularly in Europe, where there is a long legacy of mining, in order to contribute to a more sustainable circular economy [2,5,11].

Tailings have a broad range of possible applications in the industrial sector. Currently, tailings and mine wastes in general are used in the production of ceramics (e.g., roof tiles, paving stones, bricks), as aggregates in backfilling to provide stability in an underground mine or to replace voids left by extraction of the ore or as aggregates for the production of asphalt. They can also be used as secondary metal resources [10,12–18]. Investigation into metal extraction from mine wastes typically focuses on multiple rather than single elements. For example, re-processing of tailings in the Picher mining district, where Al, Ti, Pb and Zn occur in fine tailings particles and mill tailings, was found to be feasible for recovery at 2013 prices for the listed elements [19]. In another study, the Unalsky tailings were investigated and showed good recoverability for Pb, Zn, Cu, Fe and Au using hydrometallurgy metal extractions [20]. More recent studies have started to focus on the application of different mine wastes in industry, such as the use of both tailings and waste rock for metal extraction and as an additive in soils [21].

Slags produced during pyrometallurgy also have the potential for re-processing and re-use. For instance, Pioro and Pioro (2003) used slags for the production of eco-friendly building materials, based on melting aggregates with submerging combustion. They also proved that slag can be used as a filler for concrete and asphalt and as additives in the production of building materials (e.g., cement, roof tiles, brick, etc.) [22]. Kuhn and Meima (2019) characterized both tailings and slags from the Bergwerkswohlfahrt mine waste dump in order to assess their economic potential. Their study showed that 8000 t of Pb and around 17,300 kg of Ag are present in that specific mine waste dump. Taking nearby dumps into account, there may be enough material for reprocessing of the mine wastes in the future [10].

At present, most literature in this field focuses on one specific type of mine waste and either reprocessing of the material for metal extraction or for the application in the production of eco-friendly materials. This study aimed to identify the different mine waste materials present at the Plombières tailings pond (Belgium) by using a combination of geophysics and drilling. Following the classification of the different mine waste types, including both tailings and metallurgical wastes, the materials were characterized to determine potential applications of the material in the industrial sector, as a secondary resource, as well as the potential for metal recoverability. To date, there have been no characterization studies of the Plombières tailings pond, and in general, of tailings ponds produced by pyrometallurgical processing of Mississippi Valley type (MVT) ores, as is the case for the Plombières mine site [23,24]. Additionally, little or no literature has been published about the processing of the ore and deposition of the material within the tailings pond. A recent study discusses the knowledge gaps in the characterization of mine wastes

in Europe [25], which clearly demonstrates that many historic mine sites encounter the same problem.

Although detailed characterization of the Plombières tailings pond has not been performed, Kucha et al. (1996) investigated and characterized the nearby metallurgical dumps. The study focused on mineralogical, geochemical and environmental aspects of the material within the metallurgical dumps (e.g., mining waste and slags) [23]. Such studies are the first steps towards re-processing of mine waste materials, which could potentially help to meet the demand for raw materials in the European Union, leading to a lower dependency for their raw materials supply.

2. Location and History of the Plombières Tailings Pond

2.1. Site Description

Plombières is a small town located in eastern Belgium in the province of Liège. The former mining site of Plombières is located in the Plombières–Altenberg–Moresnet mining district (Figure 1). The mining district was historically important for the production of Pb and Zn in Belgium, from the beginning of mining activities in the Roman period [26] until 1922 [27]. Processing of the ore was done in Plombières, in addition to the mining. During this period, around 110,000 t of zinc ore and 115,000 t of lead ore were produced from Plombières, with an average grade of ore varying between 10 and 15% [28].
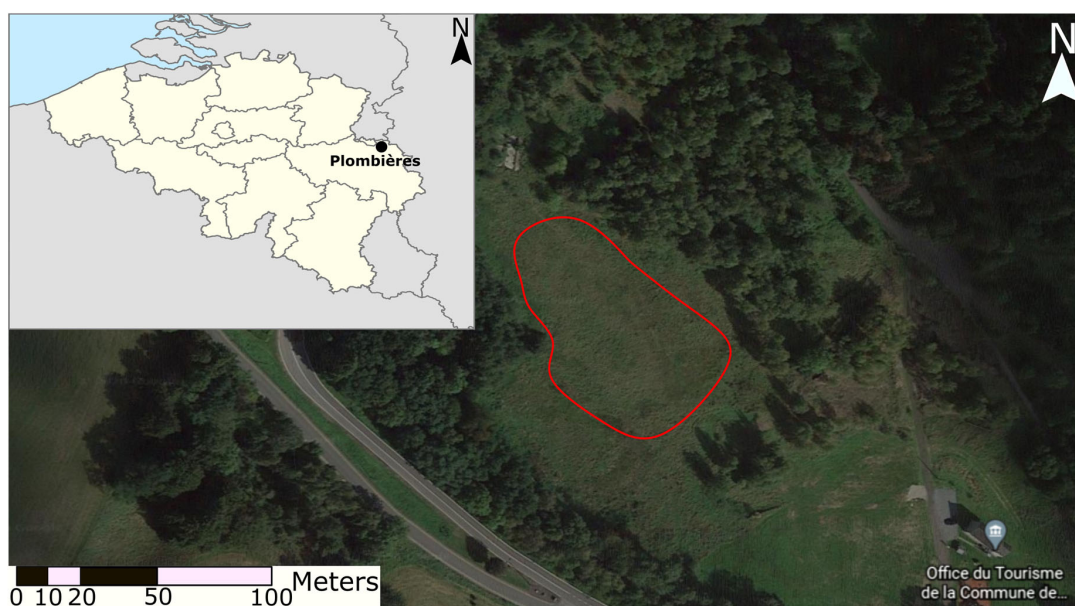
Figure 1. Map of the Plombières area showing the location of the tailings pond (Google Maps, 2019, maps.google.com.). Red polygon represents the studied area of the tailings pond.

Although the mining started in the Roman period, followed by pre-industrial mining during the Middle Ages, there was no mining activity in this area during the 17th and 18th century [29]. Mining activities reached a peak in the middle of the 19th century. During the 19th century, ores from Greece and Spain, with high concentrations of hazardous elements such as As, Hg and Cd were also imported. The mining activities ended in 1922, and in 1998, Plombières was classified as a nature reserve [27].

The tailings pond covers an area of around 8000 m², but the age of its deposition is unknown. The tailings material is covered with soils and metallurgical waste (e.g., slags) from the processing plants. Additionally, pipes that were used to melt and process the ore

are incorporated into the metallurgical waste. Despite there having been no phytoremediation at the studied site, zinc violets occur there, which is indicative of high zinc content in the soils [30].

2.2. Geological Setting of the Plombières Mineralization

The Plombières tailings were produced by the processing of Mississippi Valley-type (MVT) ore from the Plombières–Altenberg–Moresnet mining district. MVT ores are typically characterized by strata-bound Zn–Pb sulphides occurring within the carbonate host rock (e.g., karst pockets, breccias, replacing dolostones). Primary mineralogy mainly consists of sphalerite (ZnS), galena (PbS) and pyrite/marcasite (FeS$_2$). The most common gangue minerals are carbonates (calcite and dolomite) and quartz. This type of ore is most commonly exploited for metals such as Pb, Zn and Ag. MVT deposits are formed by low temperature and high salinity fluids [31,32]. The Plombières deposit itself is one of four large Zn–Pb deposits in eastern Belgium [28].

The Plombières–Altenberg–Moresnet mining district is located in the Verviers synclinorium, which formed during the Variscan orogeny [28]. The lithostratigraphic column consists, from bottom to top, of Famennian sandstone and shale, Tournaisan dolomite, Visean limestones and Namurian shales. The folded Paleozoic strata are cross-cut by NW–SE oriented faults which were active during the Mesozoic. The sulphidic Pb–Zn deposits in eastern Belgium, including Plombières, are overlain by Cretaceous sediments of the Aachen formation [33–35].

The primary mineralization assemblage comprises galena, sphalerite and pyrite/marcasite with low content of Ni and Co in the Fe sulphide minerals. The ore minerals form collomorph structures that are often brecciated [31]. Secondary phases include smithsonite, hemimorphite, willemite, cerussite, limonite and siderite, which result from the weathering of the primary ore. The main gangue minerals include carbonates, quartz and clay phases [29]. The mineralization did not extend into the Aachen formation. This indicates that emplacement of the ore happened between the end of the Variscan orogeny (ca. 295 Ma) and the Late Cretaceous (ca. 100 Ma) [36].

3. Methodology

3.1. Sampling and Sample Preparation

The tailings pond was investigated with 20 drill holes in a 40 m by 80 m grid. Sampling started with 6 exploratory drill holes that were used to constrain a grid of 15 additional drill holes (Figure 2) based on where tailings material was found, while also avoiding vegetation and slopes, where there are large amounts of whole pipes and metallurgical waste. Additionally, two pit-holes were made. Sampling was performed using a 1 m long cylinder, 8 cm in diameter, which was attached to a Ramguts hammering head. Metal extension bars of 1 m were used to sample to larger depths (up to 3.5 m). A hydraulic pumping system was used to lift the drilling bars and the sampling cylinder.

During sampling, four types of material (soil, metallurgical waste, brown tailings and yellow tailings) were defined based on their macroscopic properties, i.e., the presence of different fragments, grain size and color. Samples were taken, in intervals of 40 cm for metallurgical waste, every 20 cm for tailings material and one sample of soil per drill hole. In order to characterize the samples, they were first dried at 40 °C, which took 3 to 6 days depending on the type of material. After the samples were dried, they were de-agglomerated with a pestle and mortar and split into two increments using a riffle splitter. One split was ground to a powder (<64 μm) using a pulverizing mill for mineralogical and geochemical analysis. The second split was used for grain size measurements [37].
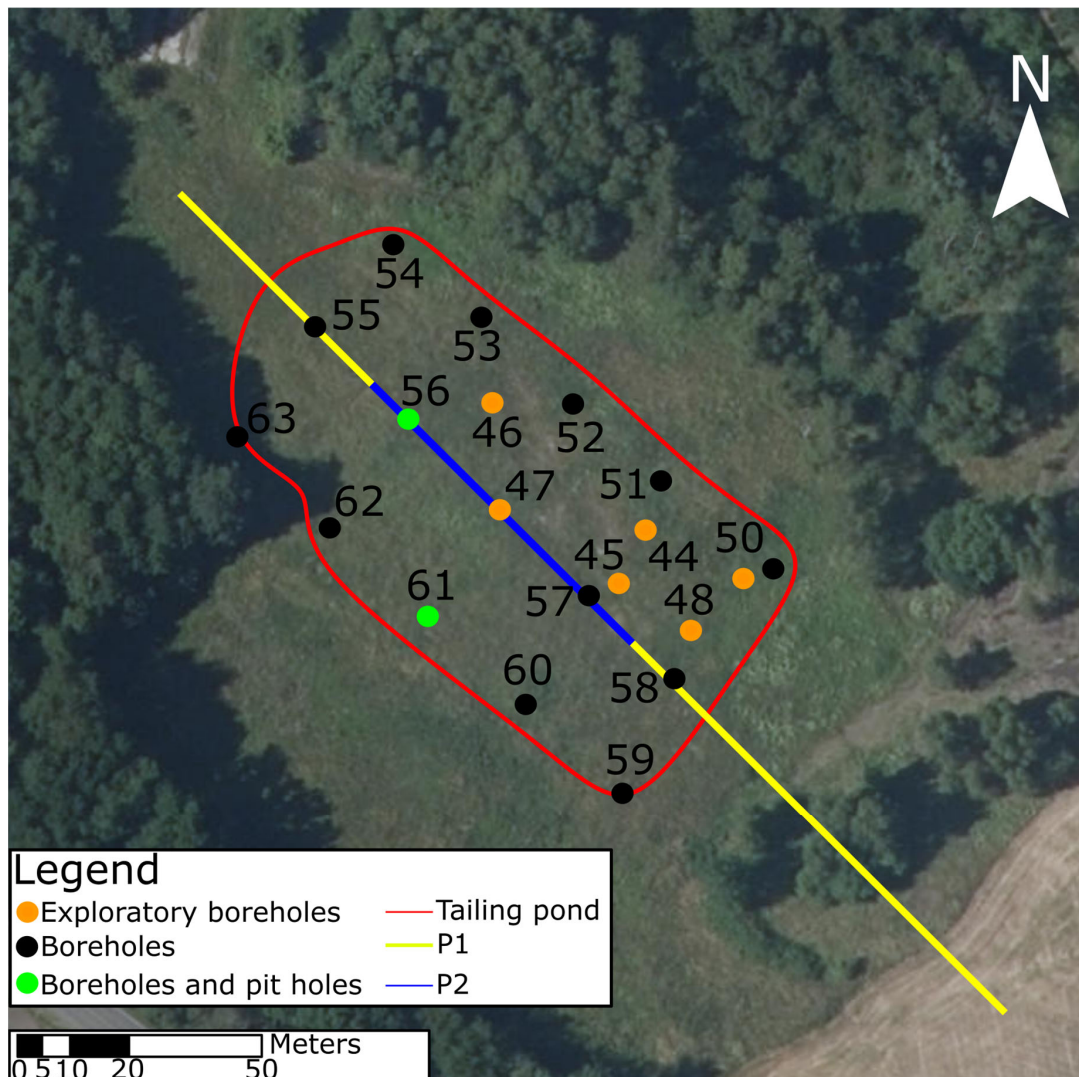
Figure 2. Map of the Plombières site, showing the orientation of the profiles studied with geophysics. The yellow line represents the short profile, and the blue line the long profile [38]. The red line represents the studied area of the tailings pond. The map also shows the sampling points. Orange dots represent the points where exploratory boreholes were made. Black dots represent the points where only drill holes were made, while green dots represent points where both drill holes and pit-holes were made [38].

3.2. Geophysical Survey

The application of geophysical techniques has been shown to be a sufficient method for exploration of the mine waste [39,40]. However, a multidisciplinary approach is needed when characterizing tailings ponds, as one single method can give misleading results [39]. Therefore, a geophysical survey was performed, combining electrical resistivity tomography (ERT) with induced polarization (IP). ERT is a non-destructive geo-electrical method that measures the electrical resistivity of the sub-surface materials. Geo-electrical characterization can be improved by measuring the chargeability, i.e., ability of a soil to polarize under an electrical field, provided by the IP method. The results depend on mineralogy, particle sizes, the porosity of the measured material and the presence of water [39].

The geophysical survey was performed to estimate the total amount of tailings material in the pond in order to assess the economic potential of the tailings pond. Additionally, geophysical surveys can allow the observation of deep internal structures of the tailings pond that cannot be reached with the shallower drill holes. In addition to ERT, other geophysical techniques can be applied for characterization of the tailing material. For example, magnetic susceptibility surveys can be used as a semiquantitative tool for the characterization of different mine wastes to make a correlation between chemical process (e.g., oxidization of pyrite) occurring within the tailings material [40].

Tomography measurements use electrode connected by a multi-core cable to an imaging system [41]. Better resolution is achieved by using short electrode spacing, but the depth that can be measured is then reduced [41,42]. For this research, a gradient configuration with a separation factor of 8 was used [41]. Two profiles with 64 equally spaced stainless-steel electrodes were deployed (Figure 2) as follows:

- A long profile—189 m long with a spacing of 3 m between electrodes (P1)
- A short profile—47.25 m long profile with a spacing of 0.75 m between electrodes (P2)

Both profiles were along the same line with an SW to NW orientation. The orientation of the profiles was chosen in order to pass through as much sampling points as possible for validation purpose. Due to logistic constraints, only these two profiles were made. Nevertheless, these two profiles provided sufficient simultaneously information on the anthropogenic deposits and the host rock at the same location. The imaging system used for data acquisition was the ABEM Terrameter LS (12 recording channels, resolution of 3 nV at 1 s integration time, ABEM, Liège, Belgium). Electrical current was injected for 1 s, and the voltage decay after the current cut off was measured for 1 s. In order to estimate data quality, measurements were repeated twice. Measurements exhibiting a repetition error larger than 5% were discarded from the dataset. Data inversion was carried out with Boundless Electrical Resistivity Tomography(BERT) using a robust constraint on the data and a smoothness constraint on the model [43]. The models obtained with BERT satisfy the error weighted chi-square, $\chi^2 = 1$, meaning that the data are fitted to their estimated error level. Among the tools available to appraise the quality of models obtained after inversion [44], the depth of investigation index (DOI) was selected to estimate the exploration depth [45]. Using DOI, the latter was estimated to around 40 m for P1 and 10 m for P2.

3.3. Laser Diffractometry

The particle size distribution of the materials found at the Plombières site was measured, using a Beckman Coulter LA 13320 laser diffraction particle size analyzer, at the Geo-Institute of KU Leuven (Leuven, Belgium). A total of 103 samples was measured. As the laser passes through a cloud of the particles to be measured, the beam encounters the particles and is scattered at an angle inversely proportional to the grain size [46,47]. The data were subsequently processed by applying the Mie scattering technique [48]. Samples were classified according to the standard Sheppard classification [49]. Prior to the measurements, the samples required removal of any cement and flocculants that might be present. The standardized "Jackson treatment" procedure was used to liberate the particles and consists of three successive steps [50]. Firstly, the carbonate cement was removed by mixing 5 g of sample with 75 mL of sodium acetate buffer and leaving the mixture overnight at room temperature. The mixture was centrifuged to separate the sample and the buffer. Again, 75 mL of sodium acetate was added to the sample and the mixture was put in an ultrasonic bath for 5 min. Afterwards, the sample-buffer mixture was heated to 80–90 °C on a hot plate and stirred for 30 min. After cooling, the mixture was once again centrifuged to remove the buffer. Secondly, organic matter was removed by mixing the sample with hydrogen peroxide and sodium acetate buffer. The sample was placed in a large beaker with 50 mL of sodium acetate buffer and heated to 70 °C. In subsequent steps,

5 mL of hydrogen peroxide was added until no reaction took place. After the reactions ceased, 10 mL of hydrogen peroxide was added, and the mixture was heated at 70 °C for three hours. After cooling, the sample-buffer mixture was centrifuged to remove the buffer. The third step involved the removal of FeO(OH), with 45 mL of sodium citrate being added to the centrifuged sample, and the mixture was heated to 75–80 °C. When the appropriate temperature was reached, 1 g of sodium dithionite was added, and after 5 min an additional 1 g was added. This was repeated once more with 2 g. After cooling, the mixture was again centrifuged to remove the sodium citrate and sodium dithionite. The samples were dried at 60 °C, and 1 g of the prepared sample was mixed with water and put in an ultrasonic bath to prevent coagulation [50,51].

3.4. X-Ray Fluorescence

Geochemical analyses were performed at the University of Liège (Liège, Belgium) using X-ray fluorescence (XRF) on a total of 115 samples. An ARL PERFORM-X 4200 XRF equipped with a Rh-tube and using a mixture of Ar-CH$_4$ gas was used for the measurements. A standard program was applied for the measurement of the 10 major elements: Si, Al, Ti, Fe, Mg, Ca, Mn, K, Na and P. Calibration curves were obtained by measuring a series of 47 to 66 international standards (rock samples with a few minerals and two soils). The UniQuant software (version 6.0) of ThermoFisher was used to detect and quantify minor and trace elements [52]. The detection limit for trace elements was 10 ppm. Glass beads were prepared for major element analyses by first drying the sample at 1000 °C for two hours in the oven. After cooling, 0.35 g of sample was mixed with 3.85 g of flux (lithium tetraborate) and LiBr (0.0020 ± 0.0002 g) and melted in a platinum crucible to form glass beads. Pressed pellets were prepared, for measuring the trace elements, by mixing 7 g of sample with 5 mL of glue (polymer consisting of C and H in solution) and acetone to prevent hardening and then hydraulically pressing the mixture to form a pellet.

3.5. X-Ray Powder Diffraction

Based on the macroscopic descriptions, the grain size and geochemical analysis, 40 representative samples were carefully selected for bulk mineralogical analysis to determine the mineralogy of the mine wastes. X-ray powder diffraction analyses were performed at the Geo-Institute of KU Leuven. The powdered sample was split using a shear splitter in order to obtain a representative sample of 1.8 g. The 1.8 g sample was subsequently mixed with 0.2 g of zincite, which was used as an internal standard. The samples were then homogenized, mixed with ethanol, milled in a McCrone micronizing mill and finally dried. The resulting powder (<64 μm) was put into a powder mount for measurement. A Philips PW 1380 diffractometer was used at a voltage of 45 kV and a current of 30 mA, and it was equipped with CuKalpha radiation, a graphite monochromator, a receiving slit width of 1 mm and a continuous scanning mode. The 2θ range was from 5° to 70° with a step size of 0.02° and a counting time of 2 s. The time of the measurements was 1 h and 40 min. Mineral phases were identified and quantified using the Profex 4.0 software, and Rietveld refinement was performed using the BGMN program [53], which is integrated into the software. In addition to XRD, samples were studied with scanning electron microscopy (SEM) at the Helmholtz Institute Freiberg (HIF) for resource technology. SEM was used to confirm the presence of different minerals and phases in the material, based on the morphology and texture of the grains, as well as their back-scattered electron (BSE) intensity. Phases with higher average atomic numbers have a higher BSE intensity and are brighter in the grey-scale images compared to phases with lower average atomic numbers. Therefore, Pb- and Zn-bearing phases could be easily distinguished by their high BSE intensity. In general, SEM has been proven to be a good method for characterization of mine wastes due to the easy identification of valuable and sulphide minerals (e.g., pyrite), which typically have a high BSE intensity, even if they are fine-grained [7].

4. Results and Discussion

4.1. Classification of Mine Waste Material Types

The mine waste materials sampled at the Plombières site were subdivided into four mine waste types: soil, metallurgical waste, brown tailings and yellow tailings (Table 1). The materials were classified based on macroscopical properties, such as color, grain size and the presence of different fragments. The results in the following sections are presented and discussed according to the defined material types.

Table 1. Macroscopic description and average thickness of the four types of material present in the drill and pit-holes at the Plombières site.

Material Type	Color	Thickness	Other Properties
Soil	Dark brown	0.1–0.2 m	Fragments of slag are often present
Metallurgical waste	Dark grey to black	0.6–1.9 m	Fragments of slag, pipes, ceramics and mortar are often present
Brown tailings	Dark brown–grey green	0.4–2.4 m	Often thin layers of weathered ceramics are noticed
Yellow tailings	Light brown–yellow–white	5.0–6.0 m *	-

* Value estimated based on geophysical measurements.

A clear vertical succession of the different materials was observed in each of the 20 drill holes and pits (Figure 3). Approximately 0.15 m of soil was found to be followed by ~1.70 m of metallurgical waste, consisting of crushed slag material, pipes that were used for smelting of the ore and building material (ceramics and mortar) of the historical factory. Due to the presence of large fragments of hard material in this layer, drilling through it was not always possible. The fragments varied in size from a few mm up to 50 cm or more. Often, the larger pieces of the pipes contained fragments of slag materials (Table 2). The metallurgical layer continued down to the brown tailings, consisting of dark brown silt material, with an average thickness of 0.8 m. Following the brown tailings was a yellow to light brown silty material, exhibiting white stains. This material was classified as yellow tailings, with the only difference to the brown tailings being the color. The average thickness of the yellow tailing could not be determined by the drill cores, since the maximum depth of the tailings exceeded the depth of drilling.

In all drill holes, the transition between layers for all types of material was clear. In several drill holes, the residue of the metallurgical processes (slags or brick material) also occurred in the upper part of the brown tailings layer. The thicknesses of the layers varied across the tailings pond (Table 1). The clear transition between layers indicated that the tailings material was deposited over time and subsequently covered by smelting pipes, slags and rubble from the processing plant. There is no documentation of when the covering of the tailings pond took place.

Figure 3. (**a**) Thin layer of soil (to the right), followed by a thick layer of metallurgical waste (**b**) Thick layer of brown tailings and transition to the yellow tailing (to the left). (**c**) One meter of yellow tailings.

**Table 2.** Information about the location, depth and type of sampling.

| ID	Coordinates		Length (m)	Type
	N	E		
44	50°44.080′	5°57.763′	0.9	Drill hole
45	50°44.076′	5°57.759′	2.5	Drill hole
46	50°44.098′	5°57.735′	0.7	Drill hole
47	50°44.082′	5°57.744′	2.4	Drill hole
48	50°44.070′	5°57.771′	1.5	Drill hole
49	50°44.076′	5°57.777′	1.0	Drill hole
50	50°44.077′	5°57.780′	1.0	Drill hole
51	50°44.085′	5°57.767′	3.5	Drill hole
52	50° 44.092′	5°57.754′	1.0	Drill hole
53	50°44.099′	5°57.740′	3.5	Drill + pit hole
54	50°44.104′	5°57.727′	1.0	Drill hole
55	50°44.095′	5°57.719′	3.5	Drill hole
56	50°44.087′	5°57.732′	2.4	Drill hole
57	50°44.075′	5°57.756′	2.4	Drill hole
58	50°44.065′	5°57.769′	1.9	Drill hole
59	50°44.057′	5°57.762′	0.9	Drill hole
60	50° 44.065′	5°57.750′	1.0	Drill hole
61	50°44.071′	5°57.737′	3.0	Drill hole
62	50°44.080′	5°57.723′	2.0	Drill + Pit hole
63	50°44.087′	5°57.708′	1.0	Drill hole

4.2. Geophysical Survey

The results of the geophysical survey, performed by combining ERT with IP, are shown in Figures 4 and 5 for the longer Profile 1 (P1) and shorter Profile 2 (P2), respectively. P1 was used to estimate the thickness of metallurgical waste and tailings and the depth to the bedrock. At approximately 8 m depth (and up to 15 m in some places), there

was a transition from low to high electrical resistivity (Figure 4a), indicating a change of lithology. Based on the resistivity characteristics of the material below this depth range and the geological maps of the Plombières deposit, the more resistive structure was interpreted to be the bedrock. The vertical resolution in this profile was too low to distinguish the four different types of the material identified during sampling and the boundaries between them. However, a large zone with high chargeability could be observed from 55 m to 155 m along the profile, with a thickness of >10 m in places. This anomaly likely delineates the extent of the deposition area and originates from the presence of electronically conductive minerals disseminated in the anthropogenic material. The small spots of higher chargeability observed from 25 m to 55 m, close to the surface, suggest the presence of other anthropogenic deposits, in addition to the main deposit, but with less vertical extent. The electrical resistivity and chargeability models also revealed vertically oriented structures centered at 105 m and 179 m. Their electrical properties differed highly from the bedrock properties. They could have been caused by collapsed mine tunnels (Rudy Swennen, pers comm. May 2020). The underground mines collapsed due to large amount of water intrusion in the underground mines. This caused the collapse of the underground mine at Plombières [54].

In Figure 5, the distribution of the four types of the material identified in the drill holes (i.e., the material units) situated near P2 are compared with geophysical results. A highly resistive and chargeable structure was found close to the surface, corresponding mainly to the metallurgical waste, as confirmed by the drill hole data. Brown and yellow tailings were also characterized by high chargeability, but with lower values. The lower resistivity (<100 Ohm.m) likely indicates a higher water content, i.e., the presence of a groundwater table. Given the relative thinness of the soil layer (0.1–0.2 m), no difference could be observed between the soil and the metallurgical waste based on the geophysics. Additionally, the electrical contrast between the brown and yellow tailings was not sufficient to differentiate these two types of material.
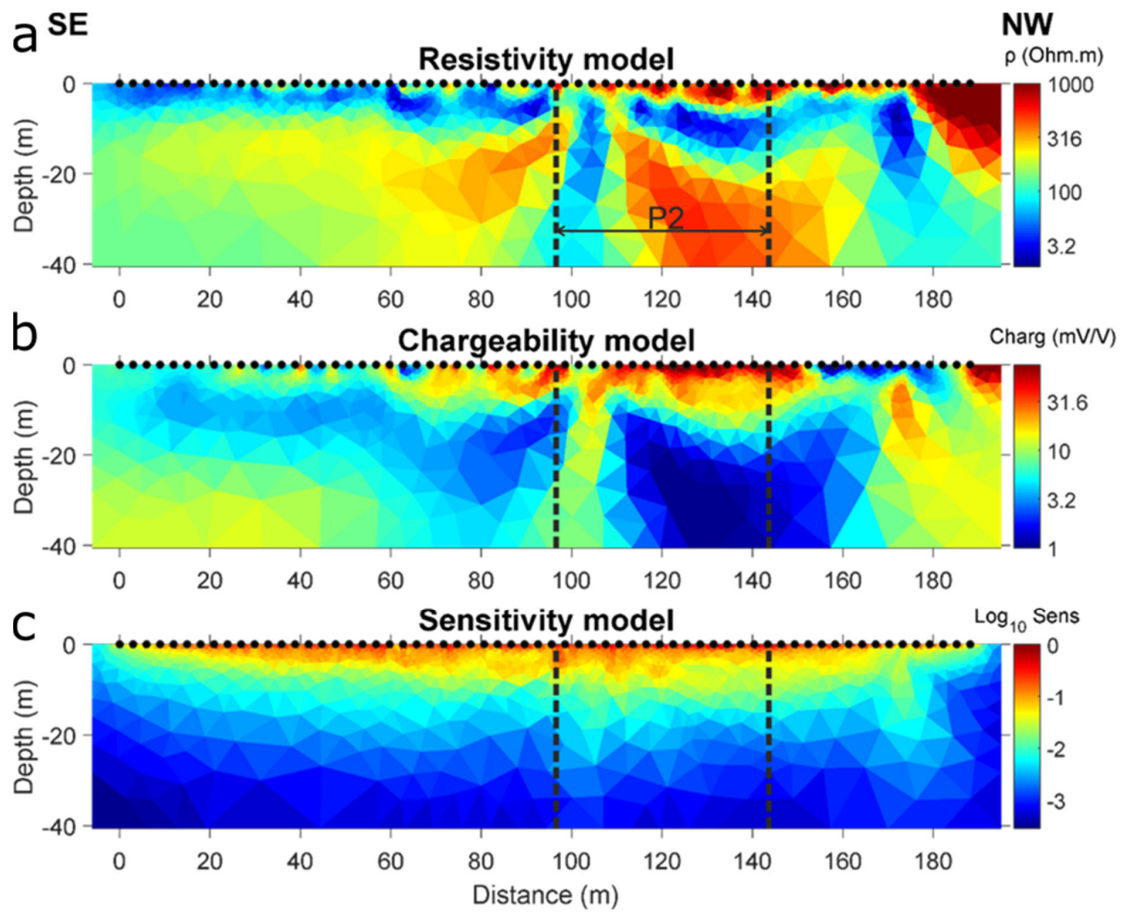
Figure 4. Inversion results for P1: (**a**) electrical resistivity model, (**b**) chargeability model and (**c**) normalized sensitivity model. The electrodes are represented by black circles. The extent of the second profile (P2) is shown by the dashed lines. Charg—Chargeability, Sens—Sensitivity.
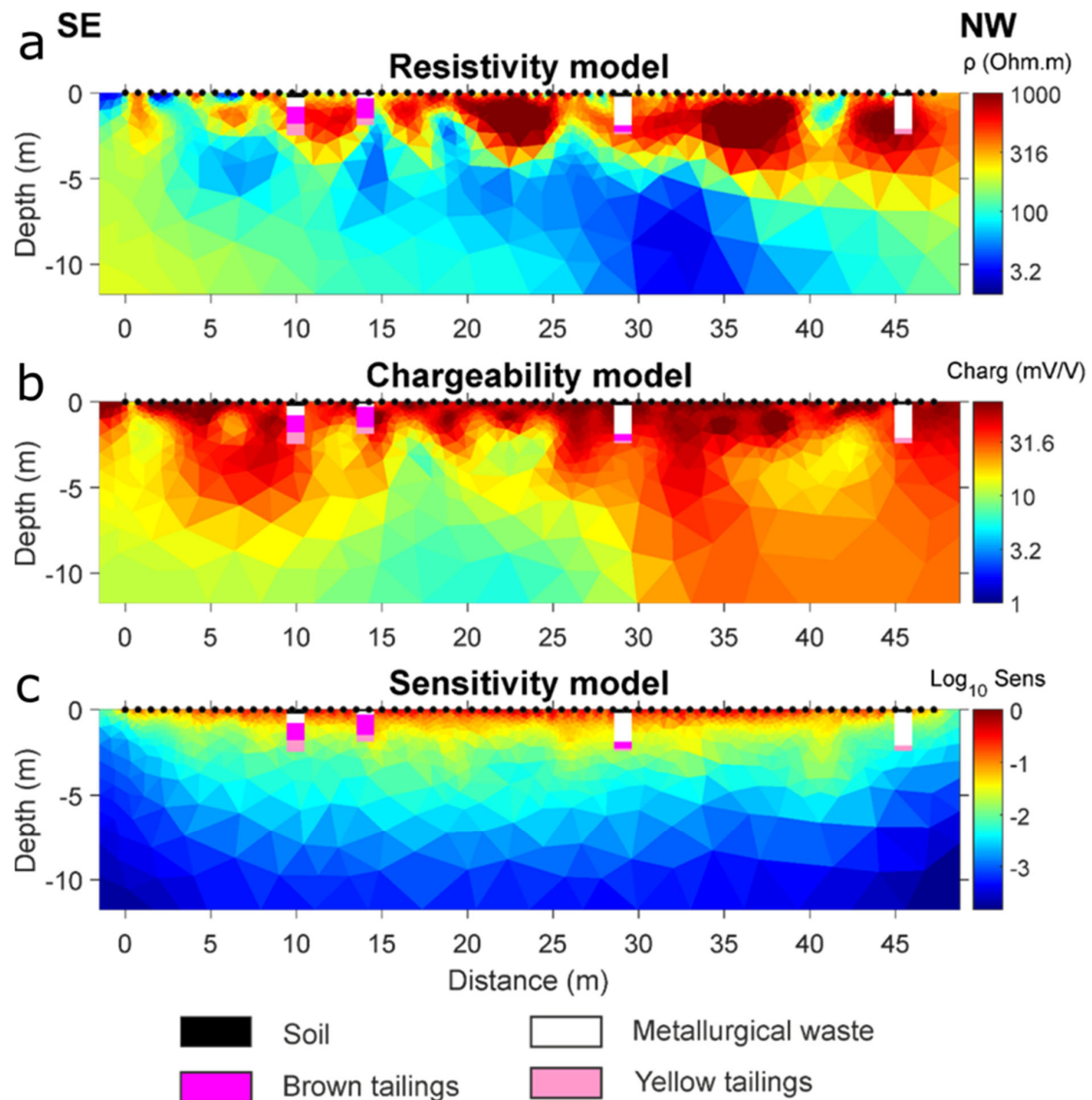
Figure 5. Inversion results for P2: (**a**) electrical resistivity model, (**b**) chargeability model and (**c**) normalized sensitivity model. The electrodes are represented by black circles. Drill holes conducted in the vicinity of the profile are also displayed for validation. Charg—Chargeability, Sens—Sensitivity.

4.3. Grain Size Distribution

For the purpose of this study, the grain size distributions of 103 samples were analyzed and classified using the Sheppard classification [50]. Based on the grain size, three sizes of fractions are defined as sand (<2 mm to 62.5 μm), silt (62.5 μm to 4 μm) and clay (<4 μm). The Sheppard classification is illustrated as a ternary diagram that defines 10 classes based on the proportions of the sand, silt and clay fractions.

Grain size analyses of the soil layer (16 samples) revealed an average distribution of 57% silt, 30% sand and 13% clay, resulting in the samples being classified as sandy silt (Figure 6). The large variation of the grain size distribution is directly related to the presence of the pyrometallurgical slags in the samples (Figure 6). During sampling and macroscopical description, the different sizes of slag fragments could be clearly seen. Most often, the slags were crushed to silt size, but occasional larger fragments, ranging from a few millimeters up to a few centimeters, were observed.

The metallurgical waste samples (33 samples) were classified as sandy silt to silty sand. The average grain size distribution of 55% silt, 33% sand and 12% clay gave an average sandy silt texture. The similarity between the soil and metallurgical waste resulted from the presence of slags, which were often present in both layers (Figure 6). Comparison with the mineralogical analyses confirmed that the samples with a more sandy grain size were indeed richer in slag phases.

The tailings layers showed less variability in the grain size distribution in comparison to the soil and metallurgical wastes. In both "brown tailings" (21 samples) and "yellow tailings" (33 samples), the most dominant fraction was silt, while the clay and sand fraction were present in similar amounts (Figure 6). The difference in the classification of the tailings while sampling was based on macroscopic properties, i.e., the clear difference in color. However, the change in the color was not accompanied by any difference in the texture of the material. This has now been confirmed by the very similar particle size distribution of the two tailings types.
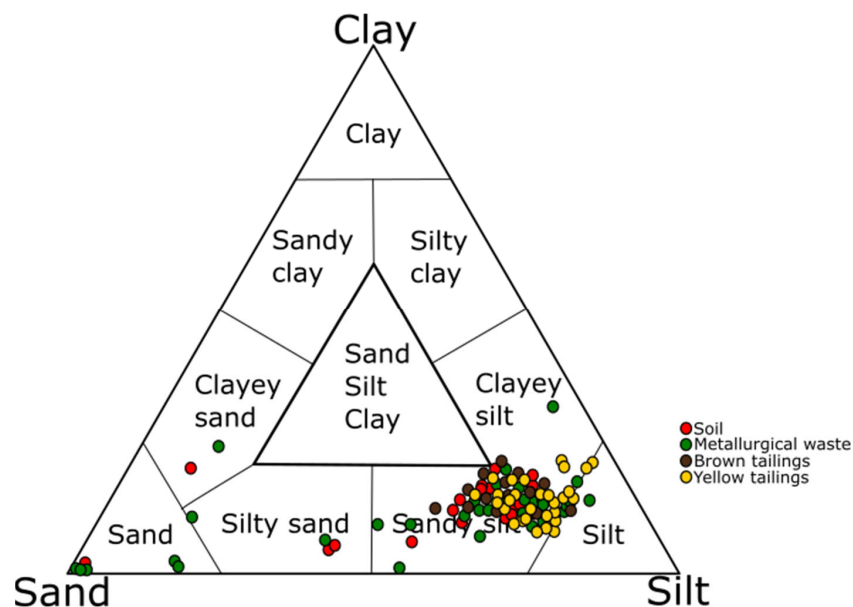
Figure 6. The grain size analysis of different anthropogenic units identified at Plombières (modified after Sheppard, 1954 [49]).

4.4. Geochemistry of Plombières Material

The results of the XRF analyses (Figure 7a–d) showed that the different mine waste materials are dominated by SiO_2 (57–77 wt.%) in term of chemical composition. The element with the second-highest concentration was aluminum (Al_2O_3), followed by elements such as Fe_2O_3, TiO_2, MnO, MgO, CaO, Na_2O, P_2O_5 and K_2O. Typically these elements occurred in the following order of abundance in all material types: Al_2O_3 (8.3–8.8 wt.%) > Fe_2O_3 (3.9–6.3 wt.%) > K_2O (1.2–1.8 wt.%) > CaO (0.4–1.3 wt.%) > TiO_2 (0.5–0.7 wt.%) ≈ MgO (0.5–0.6 wt.%) > Na_2O (0.1–0.4 wt.%) > P_2O_5 (0.1–0.3 wt.%) ≈ SO_3 (0.1–0.3 wt.%) > MnO (0.1 wt.%). Note that the range of values given represents the range of average values for the four different types of material rather than the range of all individual samples. In contrast to the previously mentioned elements, the main elements of interest, including Pb, Zn, Ga, As, Cr and Cd, followed no discernable pattern between the material types. An example of that can be observed with Pb and Zn. In soils (2.8 wt.% Pb, 3.4 wt.% Zn), metallurgical waste (2.8 wt.% Pb, 3.3 wt.% Zn) and yellow tailings (0.2 wt.% Pb, 0.2 wt.% Zn), Pb was always present in a lower concentration than Zn, whereas in the brown tailings, Pb (2.0 wt.%) had a higher content than Zn (0.8 wt.%).

Based solely on their geochemistry, soil and metallurgical waste could not be distinguished (Figure 7a,b). The samples were primarily distinguished by macroscopic observations during sampling and later on by the mineralogical composition. The similarity between these two material types implies that the soils most likely developed on the top of the metallurgical waste, since soils usually inherit the chemical properties of the parent material, which would be a metallurgical waste in this case [55]. Natural processes acting on the underlying metallurgical waste, combined with the decay of plant material, would explain the fragments of the parent material mixed with fine-grained material and the organic-rich nature of the soils [56]. There is no written evidence that the metallurgical waste was covered with soil from elsewhere. In other areas, the soil was not able to develop due to erosion by wind and water and the topographic high rather than the original depression of the pond.

The major geochemical differences observed between the soil and metallurgical waste, on one hand, and the two types of tailings, on the other hand, were the concentrations of Fe, Pb, Zn, As and Cd, which were significantly higher in the soil and metallurgical waste layers. As was below the detection limit in both brown and yellow tailings, while Cd was under the detection limit in only the yellow tailings (Figure 7e). This implies that, even if acid mining drainage were to be produced from the tailings, As and Cd are unlikely to be leached into the environment in significant quantities. The soils and metallurgical waste contained, on average, 6.2 ± 0.1 wt.% Fe, 3.3 ± 0.1 wt.% Zn, 2.8 wt.% Pb and 153 ± 2 ppm As. Although the soils and the metallurgical waste could not be distinguished based on geochemical data, the brown and yellow tailings could be distinguished based on the Pb and Zn content (Figure 7a–d). The brown tailings had metal concentrations of 1.6 wt.% Pb and 0.8 wt.% Zn, while the yellow tailings contained 0.2 wt.% of both Pb and Zn.

The Pb content in the metallurgical waste was highly variable, from a minimum of 0.1 wt.% up to a maximum of 10.1 wt.%. Similarly to Pb, Zn was highly variable in the metallurgical waste (0.1 up to 24 wt.%), as well as in the brown tailings (a few hundred ppm up to 4.0 wt.%). This high variability in the metal content could be a result of the nugget effect caused by the sampling of the material [57]. The strong heterogeneity of the material that was observed during drilling, particularly of the metallurgical waste, must also be taken into account and is likely exacerbating the nugget effect (e.g., Dominy et al., 2003 [57]). The irregular presence of fragments of metallurgical waste in the brown tailings could be contributing to the high variability in metal contents.

Based on the geochemical analyses, combined with drill core logging results, it appears that the soils, metallurgical waste and brown tailings materials are the most suitable materials for metal extraction due to their higher metal contents. With its low contents of the metals of interest, the yellow tailings could be considered as potential material for raw material for ceramics. To assess potential uses of the materials, in Section 4.8, the geochemistry results are combined with the mineralogical results and compared to regulations for ceramics production.
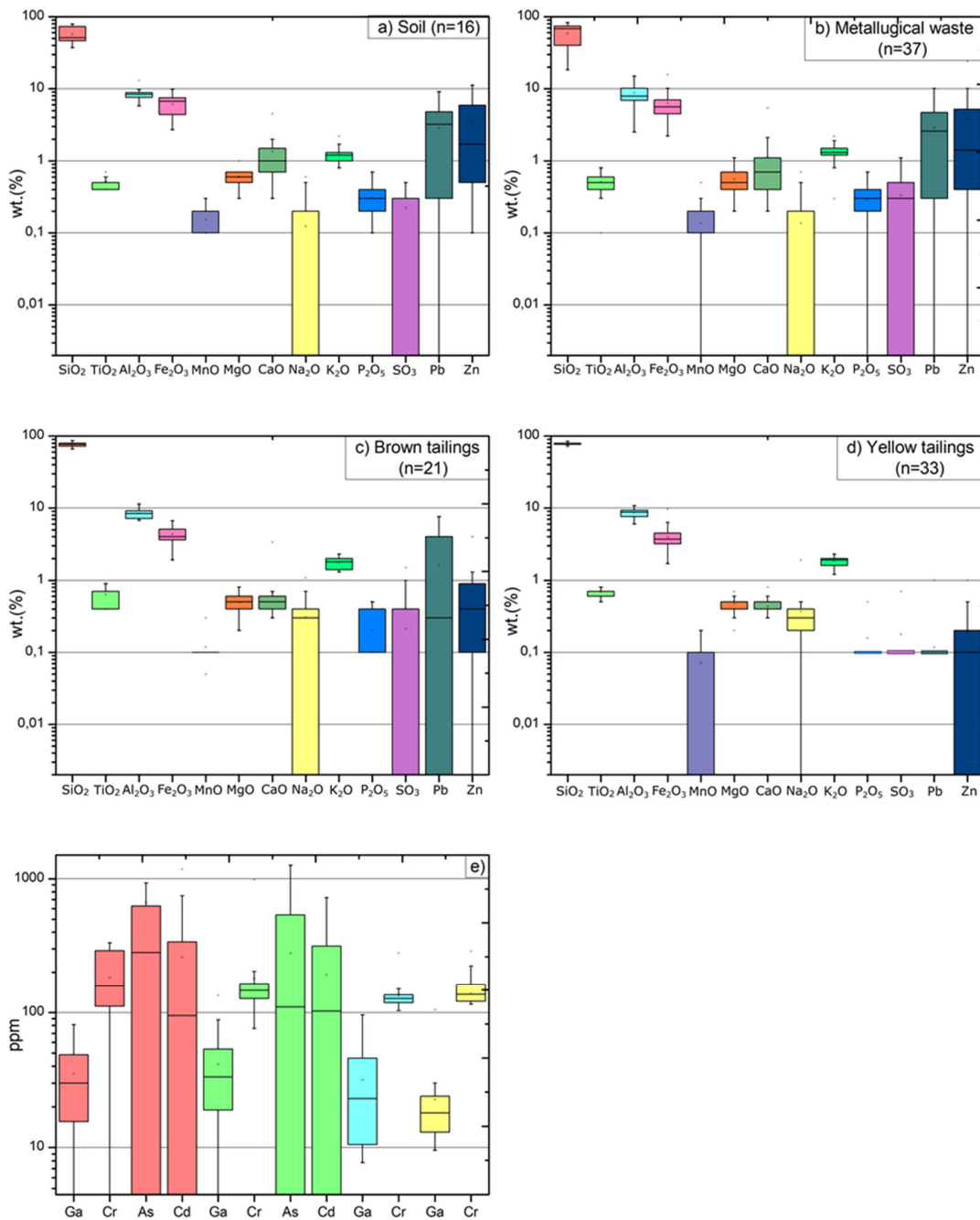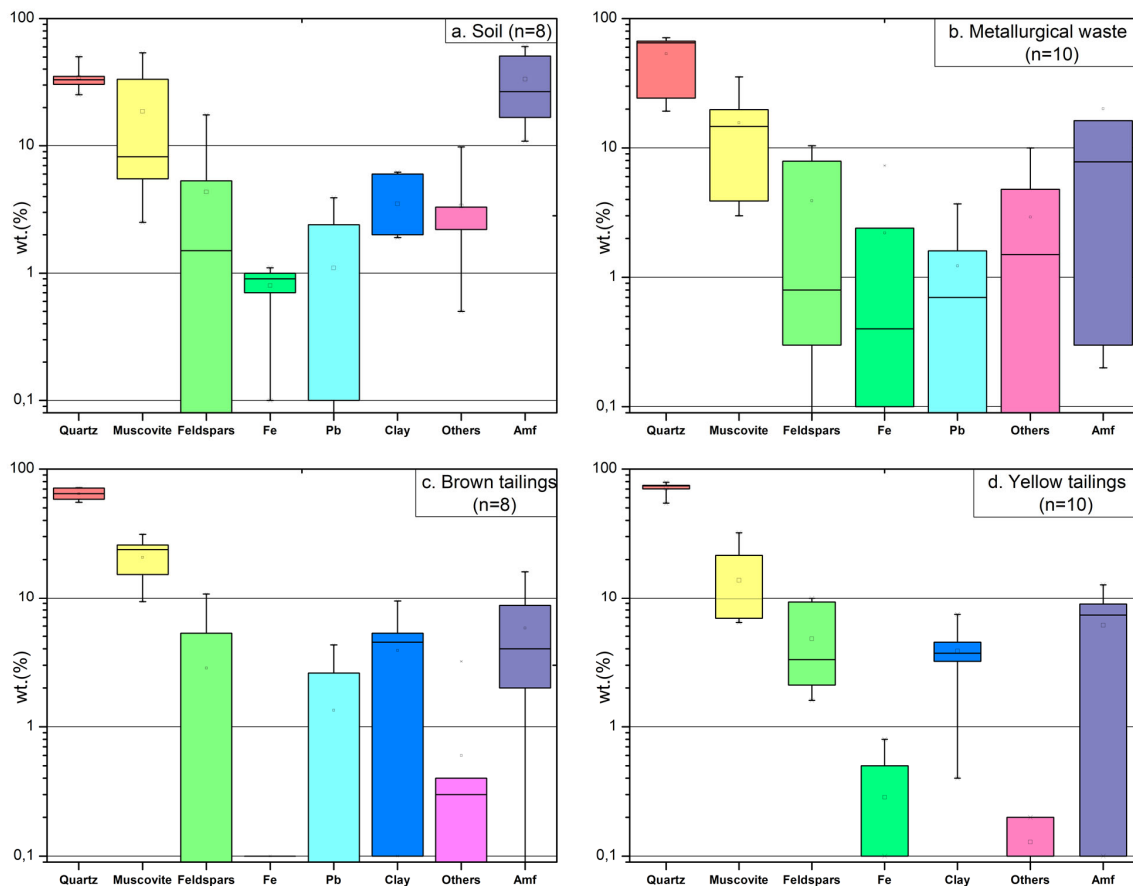
Figure 7. Whisker plots of the elemental concentrations for different anthropogenic units identified at Plombières: (**a**) soil, (**b**) metallurgical waste, (**c**) brown tailings, (**d**) yellow tailings, (**e**) values of Ga, Cr, As and Cd in the soil (red), metallurgical waste (green), brown (blue) and yellow (yellow) tailings.

4.5. Mineralogy of Plombières Materials

Mineralogical analyses of all four materials, with quantitative XRD, revealed a composition of mainly quartz (SiO_2), muscovite ($KAl_2(AlSi_3)O_{10}(OH)_2$) and amorphous phases (Figures 7 and 8a–d). Many other minerals were present in lower abundances, including feldspars (plagioclase (($NaAlSi_3O_8$–$CaAl_2Si_2O_8$) and K-feldspars (($KAlSi_3O_8$)), galena (PbS), anglesite ($PbSO_4$), cerussite ($PbCO_3$) plumbogummite ($PbAl_3(PO_4)_2(OH)5·H_2O$),

willemite (Zn_2SiO_4), chlorite (($Mg,Fe)_3(Si, Al)_4O_{10}(OH)_2 \cdot (Mg,Fe)_3(OH)_6$), goethite ($Fe^{3+}O(OH)$), cristobalite ($SiO_2$) and clay minerals.

Taking the primary ore, the host rock and processing of the ore into account, this mineralogy is consistent with the mineral phases that could be expected to be found in the Plombières materials [18]. Quartz, muscovite, feldspars, chlorite, calcite and clay minerals originate from the filling found in karst pockets. Little published information exists of the processing of the ores at Plombières. However, it is known that during the washing of the ore, light and heavy fractions were separated. The light fraction was considered to be waste and was discarded, while the heavy fraction was considered as a concentrate and was further treated. Afterwards, the ore was crushed and treated in a reverberatory furnace [58]. The light fraction from cleaning, which was disposed of, would most likely be comprised of the less dense silicate minerals, which dominate the mineralogy of the waste materials. The later pyrometallurgical processing would have produced the metallurgical waste that is found over-lying the tailings materials.

Figure 8. Whisker plots of the mineralogical composition for different anthropogenic units identified at Plombières: (**a**) soil, (**b**) metallurgical waste, (**c**) brown tailings, (**d**) yellow tailings. Fe—iron minerals (goethite, lepidocrocite); Pb—lead minerals (galena, anglesite and plumbogummite), others—chlorite, rutile, titanite and cristobalite, Amf—amorphous phase.

The soils were typically characterized by approximately equal amounts of quartz (34.5 ± 8.4 wt.%), muscovite (21.9 ± 20.5 wt.%) and amorphous phases (31.5 ± 19.2 wt.%). These three phases alone comprised more than 85 wt.% of the sample (Figure 8a). The other minerals present in soils were clay minerals, feldspars, goethite and cerussite. Similarly to the soils, the most dominant phases in metallurgical waste were quartz (53.1 ±

20.9 wt.%), muscovite (15.2 ± 11.2 wt.%) and amorphous phase (24.2 ± 20.2 wt.%) (Figure 8b). Where quartz was enriched in the samples, the color was paler and greyish, whereas the samples richer in the amorphous phase were darker in color. Other minerals present included felspars, goethite and anglesite, in significantly lower abundances.

The brown tailings varied from green–brown to dark brown in color, while the yellow tailings were light brown to light yellow with white stains. Based on the mineralogy, the two tailings types could not be differentiated by their quartz, muscovite, amorphous phase or feldspars contents. Instead, they could be distinguished by the contents of Pb- (anglesite and plumbogummite) and Fe-bearing (goethite) minerals. Brown tailings contained an average of 1.4 wt.% Pb-bearing minerals, but low contents of Fe-bearing minerals. On the contrary, Pb-bearing minerals were not identified in the yellow tailings, while the content of Fe-bearing minerals varied from 0.1 to 0.8 wt.%. The difference in color between the brown and yellow tailings is likely related to the transition from more Pb-rich and Fe-poor tailings (brown) to Pb-poor and Fe-rich tailings (yellow) as depth increases, which is reflected in the mineralogy of the tailings layers.

As previously mentioned, the waste material had high contents of amorphous phases (Figure 9a–d). They were identified in the XRD diffractograms as broad peaks with low intensities. In contrast, mineral phases produced distinct peaks when analyzed with XRD, with the intensity of the peak depending on the amount of the mineral phase present. However, the broad and low-intensity peaks of the amorphous phases can hide low-intensity peaks of mineral phases present in a small amount [59]. Therefore, the presence of the amorphous phase in the Plombières samples may have resulted in some minor and trace mineral phases being missed. Although little information can be found in the literature on how the Plombières ore was historically processed, pyrometallurgical processes were used, and therefore the amorphous phases represent smelting slag [11]. This was confirmed by the macroscopic description of the materials made during the sampling campaign, and by the shapes and textures observed by scanning electron microscopy (SEM) (Figure 10c). Helser and Cappuyns (2020) came to the same conclusion about the amorphous phases being slags when studying materials from Plombières [8].

The variability of some of the major minerals (e.g., Pb-bearing minerals in the soils, metallurgical waste and brown tailings) was very high, even within the different material types. This was associated with the high heterogeneity of the first three layers. For the soils and metallurgical waste, the heterogeneity was influenced by the presence of the slags in highly variable amounts. The soils could comprise 10 to 60 wt.% of slag, while the metallurgical waste contained from 0.2 to 60 wt.% slags. Contrary to the geochemical results, a clear difference between soil and metallurgical waste could be established. Slag was variably present, comprising between 0 and 13 wt.%. In samples where the slag was highly abundant, the muscovite content was lower (i.e., at around 6 wt.%).

The primary ore mineral found in the metallurgical waste and brown tailings was galena, which was detected with XRD and identified with SEM. Additionally, pyrite was also found to be present by SEM. As can be seen from SEM, galena was locked with anglesite or agglomerated with different minerals (Figure 10a,d), while pyrite was locked with goethite or with slag (Figure 10b).
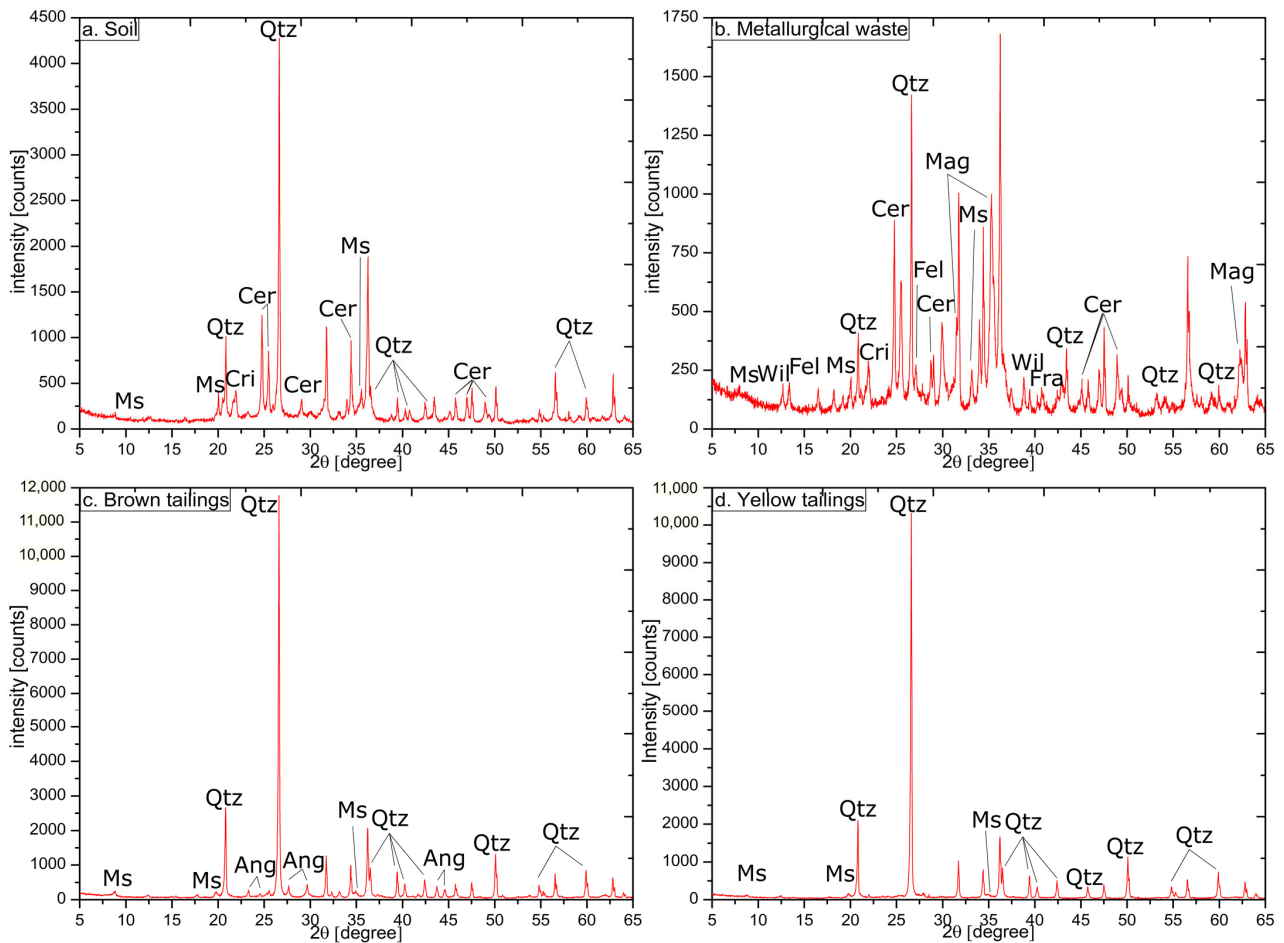
Figure 9. Diffraction spectra of the different mine waste material samples: (**a**) soil, (**b**) metallurgical waste, (**c**) brown tailings, (**d**) yellow tailings. Qtz—quartz, Ms—muscovite, Fel—feldspars, Cer—cerussite, Ang—anglesite, Cri—cristobalite, Fra—Franklinite, Wil—Willemite and Mag—magnetite. Peaks not marked are zincite, which was used as an internal standard.

Neither calcite ($CaCO_3$) nor pyrite were detected with XRD, but they were later observed with SEM (Figure 10b,d). Considering that the acid-generating minerals are encapsulated in their secondary phases, there is a small chance that they will generate acid mine drainage and the leaching of heavy metals into the environment. In contrast, grains of calcite, an acid buffer, are typically either completely or partly liberated, thus showing a potential to neutralize any acidity that could be caused by acid mine drainage [11,60,61]. Several leaching tests were performed by Helser and Cappuyns (2020) on different mine waste material from Plombières. They concluded that the highest leaching of metal(loid)s occurred under acidic and highly alkaline conditions, while metal(loid) leaching was low in neutral and alkaline conditions. The highly acidic and alkaline pHs are not likely to occur in a natural environment [8], and therefore, the potential for acidic and metal-rich waters leaching from the Plombières mine site is low.
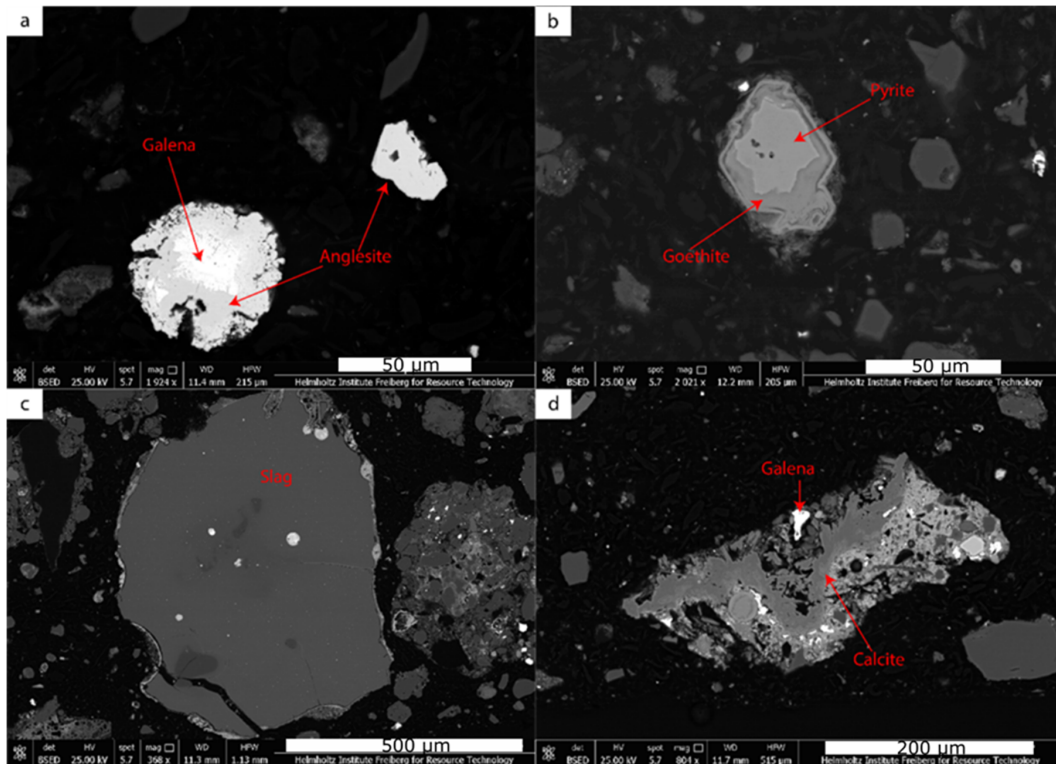
Figure 10. Photographs taken by SEM microscopy. (**a**) Composite grain of galena and anglesite. The lighter part of the grain is galena, while the darker grey part is anglesite. (**b**) Pyrite grain weathered to secondary phase (goethite). (**c**) Grain of slag with the inclusion of bright phases likely droplets of metallic phases. (**d**) Calcite grain agglomerated with grains of galena.

Overall, the mineralogical results are consistent with the geochemical analyses for all material types. Considering that quartz is the most abundant mineral in all four materials, combined with the presence of silicate minerals (e.g., phyllosilicates, feldspars), the mineralogy clearly supports that Si is the most abundant element in all samples. Aluminum mainly originates from the phyllosilicates (muscovite and clay minerals) and feldspars. Calcite and plagioclase feldspar are the sources of Ca, while K originates from phyllosilicates (muscovite and clay minerals) and K-feldspars. Other elements typically occur in low concentrations, and most likely occur in accessory minerals (e.g., P from plumbogummite, S from galena and anglesite).

4.6. Lead and Zinc Distribution

The main elements of economic interest remaining in the Plombières mine waste materials are lead (Pb) and zinc (Zn). Therefore, it is important to understand their distribution. Figure 7 exhibits the variability of the Pb and Zn contents, depending on the material, but also the high variability of these metals within the material types. As previously mentioned, the high variability of the metal concentration is due to the heterogeneity of the material, especially metallurgical waste and soils. The maximum concentrations of Pb and Zn were found to occur in the metallurgical waste > soil > brown tailings > yellow tailings. Based on the low contents of Pb and Zn, and the absence of Pb- and Zn-bearing minerals in yellow tailing (Figures 7d and 8d), it can be concluded that the separation of gangue and ore minerals and processing of the ore was efficient, even it was done a long time ago. It is unknown why there is a compositional difference between the brown and yellow tailings. It is possible that the difference may be connected to the import of Pb and Zn ore from Spain and Greece, which were rich in As, Hg and Cd [27]. However, there is no

documentation of when the tailings material derived from these ores was produced and deposited. Additionally, the geochemical analysis did not show elevated concentrations of As, Hg or Cd in the brown tailings, which could have been expected. Based on the XRD results, the Pb-bearing mineral phases present in the samples included galena, cerussite, anglesite and plumbogummite (Figure 9a–c). Anglesite and cerussite were most abundant, while galena and plumbogummite were less abundant. Anglesite and plumbogummite were dominantly present in the brown tailings (Figure 9c), while cerussite was mainly found in soils (Figure 9a).

The content of Pb present in each sample was calculated according to the stoichiometric compositions of the Pb-bearing minerals and their concentration. The same calculation was made for the samples in which Zn-bearing minerals were identified. It can be seen in Figure 11 that the correlation between the Zn and Pb contents measured with XRF and those calculated from the XRD results is low. This could be due to the under-estimation of the contents of the Pb- and Zn-bearing phases, as well as other Pb- and Zn-bearing phases present not being identified by XRD. Additionally, the amorphous phases, mostly slags, most likely contain Pb and Zn. Kucha et al. (1996) performed analyses on samples from the metallurgical waste dumps originating from the Plombières smelting process. They found that the slags are mainly Si slags, but also metal-bearing slags occur, containing Fe (30–46 wt.%), Mn (0.9–1.1 wt.%), Zn (1.5–4.3 wt.%) and Pb (1.7–2.2 wt.%) [24]. The Pb content in the slags was distributed between inclusions of Pb-bearing minerals (e.g., galena), lead droplets within the slags and Pb incorporated into the amorphous structure of the slags [24]. These observations are supported by the findings of this study, where galena and anglesite were found as inclusions in the slags (Figure 10c).
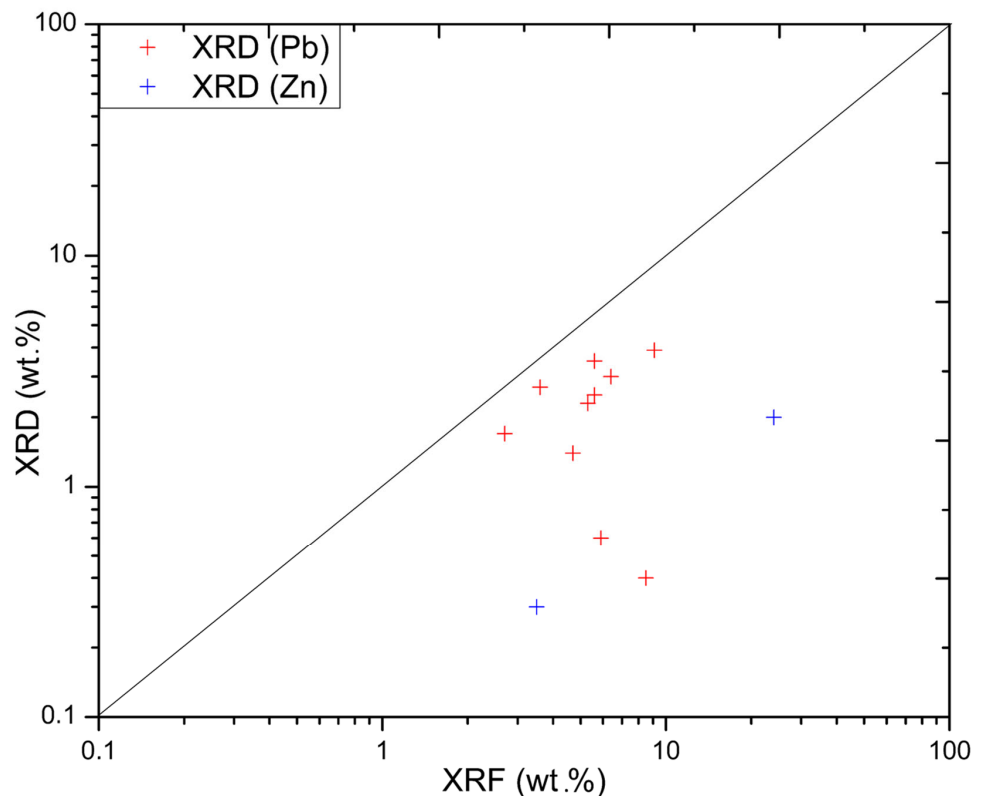

Figure 11. Scatter plot of Pb (red) and Zn (blue) values calculated from XRD versus the Pb and Zn values measured with XRF. Only samples where the Pb or Zn minerals were found were plotted. The underestimation of the Pb and Zn contents, based on XRD, are clearly shown.

Based on the results of this study, Pb is dominantly present in anglesite and cerussite, as well as in the slag phases. This is in agreement with the findings of Kuhn and Meimam (2019), Moles (2004) and Pascaud (2014), who described anglesite as a major lead source in historic tailings, as well as several other phases such as cerussite, beudanitete and Fe-oxyhydroxide [10,62,63]. Zn is assumed to mostly be present in the slag phases, with small amounts of Zn-bearing minerals present.

4.7. A 3D Model and Resource Estimation of the Plombières Site

A 3D model of the studied area of the Plombières site was constructed based on the drill core logging and the geophysical profiles (Figure 12). Progressive deposition of the tailings material inside the tailings pond resulted in clear contact between the different layers, as seen when logging the drill cores. After approximately the first 2 m of cover material, around 6 m of tailings material are present, according to the results of the geophysical survey. Considering the average thickness of the tailings material and the gridded and sampled surface of the Plombières site (3200 m²), the total volume of this area is 19,200 m³. The authors could find no information on the total area of the tailings pond in the literature, but according to the shape of the Plombières site, the estimated surface of the pond is approximately 8000 m² (Figure 12). Taking into account an estimated surface of 8000 m² and an average thickness of 6 m for the tailing material, the total volume is likely to be around 48,000 m³.
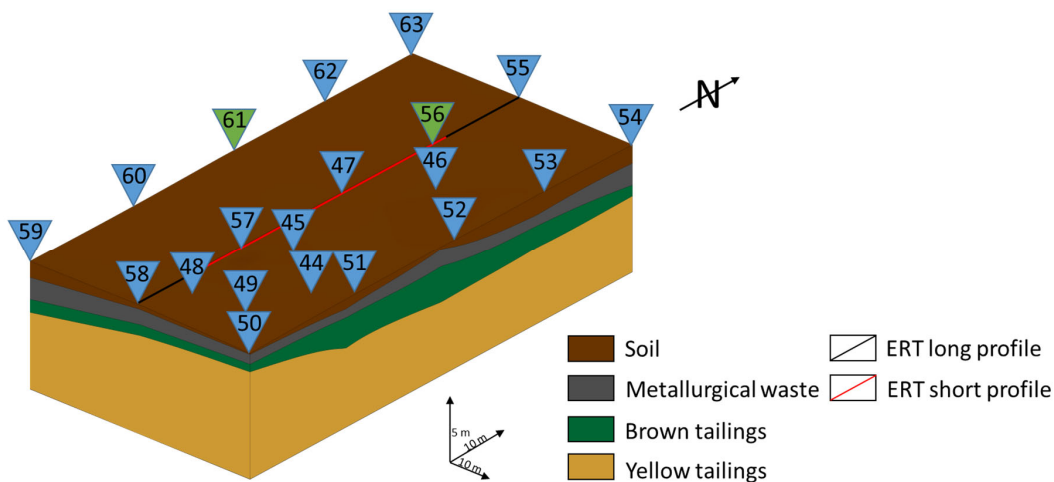
Figure 12. A 3D model of the distribution of the cover and tailings material at the Plombières site based on drill core logging and the geophysical profiles. Blue triangles represent drill hole locations, and green triangles represent the locations where both a pit-hole and a drill hole samples were taken.

A simple resource estimation of the Plombières mine waste was performed based on the data obtained in this study, including the volumes of the material layers and their metal contents. Although the highest contents of the metals of interest occur in the soils (2.8 wt.% Pb, 3.4 wt.% Zn) and metallurgical waste (2.8 wt.% Pb, 3.3 wt.% Zn) layers, the brown tailings also have a reasonably high content of metals (2 wt.% Pb and 0.8 wt.% Zn). The yellow tailings layer, despite being the thickest layer (Table 1), has low metal contents (0.2 wt.% Pb and 0.2 wt.% Zn) and therefore it is unlikely that any metals could be recovered economically. However, individual material types are not suitable for mining separately. For instance, in order for the brown tailings to be accessed, the metallurgical waste must first be removed. Therefore, the grades and volumes of metals in these two layers were combined for the estimation of an overall tonnage (Table 3). The overall Pb and Zn grades for the two layers were calculated, with a weighting based on the thickness of the layers, as 2.4 wt.% Pb and 3.5 wt.%.

The estimation of the metal tonnages first required estimation of the densities of the layers of the resource potential and the bulk density of the metallurgical waste. The bulk density of the metallurgical waste was estimated to be 1.3 t/m³, this being the mean value given for polymetallic (Pb, Cu, Zn, Cr, Fe) metallurgical waste by Kicinska (2020). For both tailings layers, the bulk density was assumed to be 2.0 t/m³, according to the review of Kuhn and Meima (2019), who based the average density on several articles [10,64]. Accordingly, the total tonnages of Pb and Zn in the metallurgical waste and brown tailings were estimated to be 279.9 t and 373.3 t, respectively

Table 3. Theoretical tonnages and metals content in the Plombières tailings pond. MW—metallurgical waste; BT—brown tailings; YT—yellow tailings.

Material	Area (m²)	Thickness (m)	Volume (m³)	Density (t/m³)	Tonnage (ton)	Pb (wt.%)	Zn (wt.%)	Pb (wt.%)	Zn (wt.%)	Tonnage (t)	Pb (t)	Zn (t)	Pb (t)	Zn (t)
MW	3200	1.7	5440	1.3	7072	2.8	4.7	2.4	3.5	12,192	198.0	332.4	279.9	373.3
BT	3200	0.8	2560	2.0	5120	1.6	0.8				81.9	41.0		
YT	3200	5	16,000	2.0	32,000	0.2	0.2	0.2	0.2	32,000	64.0	64.0	-	-
-			MW + BT + YT			-	-	0.9	1.3	44,192	-	-	343.9	437.3

According to the typical mineral resource classification schemes (e.g., The Australasian Code for Reporting of Exploration Results, Mineral Resources and Ore Reserves (JORC), NI 43-101, The Pan European Reserves and Resources Reporting Committee (PERC), etc.), the estimate made here would be "inferred resources" due to the high uncertainty of the estimates [65]. This resource estimation is highly simplified since it is based only on the estimated volumes of the mine waste layers and the corresponding metal grades, without taking other modifying factors into account, such as recoverability of the metals, mineral processing method, social license to operate, etc. In particular, it would be important to first investigate the deportment of Pb and Zn and the textural properties of the Pb- and Zn-bearing phases, such as liberation, which would strongly control the potential recoverability of the metals by any processing method. For instance, slag phases are a major source of Pb and Zb, which makes the extraction of metals more challenging due to the need for different processing methods. Different processing routes may be necessary for the material types due to the variation in grain size and composition between the layers. For example, the metallurgical waste and soils are coarser-grained and would require milling to reach a similar grain size to the brown tailings, which would increase the processing costs. Based on the calculated tonnage, the amount of the material is too low for economic extraction of the metals.

4.8. Implications for Application in the Ceramic Industry

The necessity to increase the re-use of mine waste materials in order to move towards a more circular economy has led to many examples of tailings materials being used as aggregates or additives in industrial materials, such as cemented paste backfill [66], geopolymer bricks [67] or housebuilding material (e.g., ceramic tiles) [68]. The low contents of metals and hazardous elements combined with the high amount of silicate minerals in the Plombières mine wastes, especially the yellow tailings, are a good indication that the material could be used in the production of building materials [69]. The Plombières yellow tailings could be considered as metal-poor silt tailings.

Before a material can be used in the building industry, it must satisfy certain standards, for example, the "Flemish regulation on sustainable management of materials cycles and waste" (VLAREMA) [70], the requirements for metal concentrations of which are presented in Table 4. When the concentrations of certain elements exceed the thresholds, the samples should be tested for leaching and cleaning. The values of metals specified in the regulations were compared with the metal concentrations of the Plombières tailings (Table 4). The yellow tailings were found to be more suitable for the production of the building material than the brown tailings, although the values of both Pb and Zn are slightly

above the maximum values as specified in VLAREMA (2012) [70]. The purity of the material also influences the ratio of the material that can be used for production. The cleaner the material is, the greater the amount that can be used in production without any additional cost that might come with the cleaning of the material (VLAREMA, 2012) [70]. Either the tailings materials from Plombières would need to be cleaned to reduce their contents of hazardous elements (increasing the production cost), or they would need to be used in small amounts in the ceramics.

The metal content, mineralogy and grain size influence the properties of ceramics [71]. For ceramic production, the preferred size fraction is clay, rather than silt and sand, to improve the quality of the ceramic products (e.g., strength, resistance to weathering, porosity, etc.) [72]. In contrast, properties such as coefficients of thermal expansion and electrical conductivity benefit from a coarser grain size [73]. The Plombières tailings are dominantly silt sized, which makes them suitable as a raw material for ceramic production without requiring additional grinding, which lowers the price of production.

Preliminary testing on the production of roof tiles showed good results when incorporating 5%, by mass, of the Plombières tailings into the production mixture [74]. Despite the preliminary testing showing good results, the amount of tailings material available (40,000 m³), combined with the Zn- and Pb-rich cover material, hinders the extraction of the material.

Table 4. Maximum metal and hazardous element contents in the material used for the production of ceramics according to VLAREMA (2012) [70] compared with average values of the metallurgical waste, brown and yellow tailings materials at Plombières.

Metal	VLAREMA, 2012 (ppm)	Metallurgical Waste (ppm)	Brown Tailings (ppm)	Yellow Tailings (ppm)
As	250	220	<10	<10
Cd	10	176	<10	<10
Cr	1250	160	126	139
Pb	1250	28,000	19,768	1725
Zn	1250	33,000	7528	1912

5. Conclusions

The Plombières site mine waste materials, as with many other historic mine sites, contain elevated concentrations of valuable metals. The minimum surface area of the tailings pond is approximately 8000 m². Geophysical measurements combined with drill core logging show that the average thickness of the two types of tailings (brown and yellow) is 6 m, which is covered with 2 m of metallurgical waste (slags, pipes used for the smelting of ores and building material from the washing plant) and soils. A recent drilling campaign (August 2020), with several boreholes up to 5 m deep, confirmed that the yellow tailings are continuously present until 5 m depth in the tailings pond. Cover material shows a range of textures, from sand (sand > silt) to sandy silt (sand < silt), while the clay content is constant. Soil and metallurgical waste samples contain high amounts of SiO_2 (≈58 wt.%). The total metal content (Fe, Pb, Zn) is, on average, around 12.3 wt.% in the soil and 12.6 wt.% in the metallurgical waste. Fe is the most abundant metal (≈6.2 wt.%), followed by Zn (≈3.4 wt.%) and Pb (≈2.8 wt.%). The most dominant minerals are quartz and muscovite, which is consistent with the geochemical results, i.e., SiO_2, Al_2O_3 and K_2O are the main elements. The most dominant size fraction in the tailings is silt, followed in equal proportions by sand and clay. Both types of tailings present in the Plombières tailings pond contain significant amounts of SiO_2 (≈77 wt.%), Al_2O_3 (≈8.5 wt.%), K_2O (≈1.8 wt.%) and Fe_2O_3 (≈4 wt.%). Quartz, muscovite and slags are the most abundant phases. The largest differences observed between the two types of tailings are seen in the Pb and Zn contents, as well as in the color. The brown tailings have higher concentrations of Zn (≈0.4 wt.%) and Pb (≈1.6 wt.%) than the yellow tailings (Zn ≈ 0.2 wt.%; Pb ≈ 0.2 wt.%). The main metals of interest in the studied mine wastes are Pb and Zn. They are found to occur in

both primary (e.g., galena) and secondary (e.g., anglesite) minerals. The high content of amorphous phases is associated with metallurgical slags.

A resource estimate was made based on the volumes of the material layers and their metal contents. It was concluded that it would be most economically viable to extract Pb and Zn from both the metallurgical waste and brown tailings due to the thickness of these layers and their metal contents. The tonnage was calculated theoretically as the amount of Pb and Zn in the metallurgical waste and brown tailings layers. The total tonnages of Pb and Zn in the metallurgical waste and brown tailings are estimated to be 279.9 t of Pb and 373.3 t of Zn. Despite the contents of metals remaining in the mine wastes, the potential for exploitation is hampered by the classification of the Plombières area as a nature reserve. Such factors should also be included in mineral resource estimates as modifying factors [64], since this means that legislation would make it difficult to get the required licenses for mining. Additionally, the whole area of Plombières is known for tourism and agriculture.

When the geochemistry of the different mine waste materials were compared to the Flemish regulations on sustainable management of material cycles and waste (VLAREMA)[70], it was concluded that only the yellow tailings are suitable to be used as supplementary material for the production of eco-friendly ceramics. In contrast, the elevated content of metals in the metallurgical waste (As, Cd, Cr, Pb and Zn) and brown tailings (Pb and Zn) exceed limits given by the legislation. Although the yellow tailings are potentially suitable, the low amount of material and the Zn- and Pb-rich cover hinder the exploitation of the material.

Acid-generating minerals (pyrite and galena) are entrapped in their secondary phases or in slag phases. This reduces the potential for the generation of AMD and the leaching of heavy metals into the environment. Additionally, acid-buffer minerals (calcite) are liberated, which means that any acidity caused by acid mine drainage could be neutralized. This indicates that the Plombières tailings pond represents a relatively low environmental threat. However, the abundance of heavy metals in the material, which were identified in this study, is still significant and therefore should be monitored as a potential hazard for the environment.

Better understanding of Pb and Zn deportment is necessary for improved assessments of the recoverability of Pb and Zn in the Plombières mine wastes. Therefore, additional methods will be used for characterization in the future, including mineral liberation analysis (MLA) and electron microprobe analysis (EPMA). Based on the overall assessment, further research will be focused on potential extraction methods (e.g., hydrometallurgy) as well as more advance characterization of the materials.

Author Contributions: S.B. conducted sampling and geophysical measurements, followed by petrographical, geochemical (XRF) and mineralogical (XRD and grain size distribution) analysis. He prepared the manuscript and compiled and processed data. R.B. proof-read the manuscript and advised on content and discussions. J.V.A. contributed with selecting an optimal program from geochemical measurements and the interpretation of the results. She reviewed the article with a special focus on the geochemistry. N.D. carried out part of the preparation of samples for the XRF analysis and all instrumental XRF analysis. He reviewed the paper with a focus on the geochemical methodology. D.C. lead the geophysical field campaign and performed the interpretation of the geophysical data. He read the article with a special focus on the geophysical analysis. F.N. proposed and discussed the optimal method for the geophysical method to be used and for the interpretation of the tailings pond. He reviewed the paper with special attention to the geophysical analysis. P.M. proposed the research project and initiated the research at Plombières. He organized and participated in the fieldwork and contributed to the interpretation of all data. He reviewed several times the manuscript and discussed it with the first author. All authors have read and agreed to the published version of the manuscript.

Institutional Review Board Statement: Not applicable.

References

1. European Commission. *Study on the EU's list of Critical Raw Materials—Final Report*; European Commission: Brussels, Belgium, 2020.
2. Falagán, C.; Grail, B.M.; Johnson, D.B. New approaches for extracting and recovering metals from mine tailings. *Miner. Eng.* **2017**, *106*, 71–78, doi:10.1016/j.mineng.2016.10.008.
3. Ceniceros-Gómez, A.E.; Macías-Macías, K.Y.; De La Cruz-Moreno, J.E.; Gutiérrez-Ruiz, M.E.; Martínez-Jardines, L.G. Characterization of mining tailings in México for the possible recovery of strategic elements. *J. South Am. Earth Sci.* **2018**, *88*, 72–79, doi:10.1016/j.jsames.2018.08.013.
4. Martinez, J.M.R.; Hidalgo, M.; Rey, J.; Garrido, J.; Kohfahl, C.; Benavente, J.; De Rojas, D.H.F. A multidisciplinary characterization of a tailings pond in the Linares-La Carolina mining district, Spain. *J. Geochem. Explor.* **2016**, *162*, 62–71, doi:10.1016/j.gexplo.2015.12.013.
5. Hudson-Edwards, K.; Jamieson, H.; Lottermoser, B.G. Mine Wastes: Past, Present, Future. *Elements* **2011**, *7*, 375–380, doi:10.2113/gselements.7.6.375.
6. Ettler, V. Soil contamination near non-ferrous metal smelters: A review. *Appl. Geochem.* **2016**, *64*, 56–74, doi:10.1016/j.apgeochem.2015.09.020.
7. Jamieson, H.E.; Walker, S.R.; Parsons, M.B. Mineralogical characterization of mine waste. *Appl. Geochem.* **2015**, *57*, 85–105, doi:10.1016/j.apgeochem.2014.12.014.
8. Helser, J.; Cappuyns, V. Trace elements leaching from Pb-Zn mine waste (Plombières, Belgium) and environmental implications. *J. Geochem. Explor.* **2020**, *106659*, 106659, doi:10.1016/j.gexplo.2020.106659.
9. Environment Agency. *Human Health Toxicological Assessment of Contaminants in Soil*; (England and Wales); Environment Agency: Bristol, UK, 2009.
10. Kuhn, K.; Meima, J.A.; Kuhn Characterization and Economic Potential of Historic Tailings from Gravity Separation: Implications from a Mine Waste Dump (Pb-Ag) in the Harz Mountains Mining District, Germany. *Minerals* **2019**, *9*, 303, doi:10.3390/min9050303.
11. Lottermoser, B.G. *Mine Wastes: Characterization, Treatment and Environmental Impacts*, 3rd ed.; Springer: Berlin/Heidelberg, Germany, 2003; p. 400.
12. Terrones-Saeta, J.M.; Suárez-Macías, J.; Iglesias-Godino, F.J.; Corpas-Iglesias, F.A. Development of Porous Asphalt with Bitumen Emulsion, Electric arc Furnace Slag and Cellulose Fibers for Medium Traffic Roads. *Minerals* **2020**, *10*, 872, doi:10.3390/min10100872.
13. Lam, E.J.; Zetola, V.; Ramírez, Y.; Montofré, Í.L.; Pereira, F. Making Paving Stones from Copper Mine Tailings as Aggregates. *Int. J. Environ. Res. Public Health* **2020**, *17*, 2448.
14. Suárez-Macías, J.; Terrones-Saeta, J.M.; Iglesias-Godino, F.J.; Corpas-Iglesias, F.A. Retention of Contaminants Elements from Tailings from Lead Mine Washing Plants in Ceramics for Bricks. *Minerals* **2020**, *10*, 576, doi:10.3390/min10060576.
15. Büttner, P.; Osbahr, I.; Zimmermann, R.; Leißner, T.; Satge, L.; Gutzmer, J. Recovery potential of flotation tailings assessed by spatial modelling of automated mineralogy data. *Miner. Eng.* **2018**, *116*, 143–151, doi:10.1016/j.mineng.2017.09.008.
16. Thomassen, B. The Blyklippen lead-zinc mine at Mesters Vig, East Greenland. *Geol. Ore* **2005**, *5*, 12.
17. Sukhoon, P.; Million, T.; Hyeong-Ki, K. *The Applications of Mine Tailings to Develop Low-Cost UHPC*; International Interactive Symposium on Ultra-High Performance Concrete; Iowa State University Digital Press: Iowa, USA, **2016**; doi:10.21838/uhpc.2016.92.
18. Moran, P.; Christoffersen, L.; Gillow, J.; Hay, M. Cemented Tailings Backfill—It's Better, Now Prove It! In Proceedings of the SME Annual Meeting, Denver, CO, USA, 24–27 February 2013.
19. Andrews, W.J.; Moreno, C.J.G.; Nairn, R.W. Potential recovery of aluminum, titanium, lead, and zinc from tailings in the abandoned Picher mining district of Oklahoma. *Miner. Econ.* **2013**, *26*, 61–69, doi:10.1007/s13563-013-0031-7.
20. Evdokimova, S.I.; Evdokimova V.S. Metal Recovery from Old Tailings. *J. Min. Sci.* **2014**, *50*, 800–808. © *Original Russian Text, Fiziko-Tekhnicheskie Problemy Razrabotki Poleznykh Iskopaemykh*; Pleiades Publishing, Ltd.: Russia, 2014; pp. 172–182.

21. Mehta, N.; Dino, G.A.; Passarella, I.; Ajmone-Marsan, F.; Rossetti, P.; De Luca, D.A. Assessment of the Possible Reuse of Extractive Waste Coming from Abandoned Mine Sites: Case Study in Gorno, Italy. *Sustainability* **2020**, *12*, 2471, doi:10.3390/su12062471.

22. Pioro, L.; Pioro, I. Reprocessing of metallurgical slag into materials for the building industry. *Waste Manag.* **2004**, *24*, 371–379, doi:10.1016/s0956-053x(03)00071-0.

23. Kucha, H.; Martens, A.; Ottenburgs, R.; De Vos, W.; Viaene, W. Primary minerals of Zn-Pb mining and metallurgical dumps and their environmental behavior at Plombières, Belgium. *Environ. Earth Sci.* **1996**, *27*, 1–15, doi:10.1007/bf00770598.

24. Dejonghe, L.; Ladeuze, F.; Jans, D. Atlas des gisementsplombo-zincifères du Synclinorium de Verviers (Est de laBelgique). *Mémoire l'Explication Géologique Minières Belgique* **1993**, *33*, 1–483.

25. Blasenbauer, D.; Bogush, A.; Carvalho, T.; Cleall, P.; Cormio, C.; Guglietta, D.; Fellner, J.; Fernández-Alonso, M.; Heuss-Aßbichler, S.; Huber, F.; et al. Knowledge base to facilitate anthropogenic resource assessment. Deliverable of COST Action Mining the European Anthrothropogenic Resource Assessment. *Zenodo* **2020**, doi:10.5281/zenodo.3739164.

26. Renson, V.; Fagel, N.; Mattielli, N.; Nekrassoff, S.; Streel, M.; De Vleeschouwer, F. Roman road pollution assessed by elemental and lead isotope geochemistry in East Belgium. *Appl. Geochem.* **2008**, *23*, 3253–3266, doi:10.1016/j.apgeochem.2008.06.010.

27. Dejonghe, L. *Plomb'hier a bonnes mines, Montzen: ASBLE space Culture-Plombières*; ASBLE space Culture: Montzen, Belgium, **2014**. 1, 12.

28. Dejonghe, L. Zinc-lead deposits of Belgium. *Ore Geol. Rev.* **1998**, *12*, 329–354.

29. Blondieau, M.; Polrot, F. Les travaux miniers de schimper, siège sud de la mine du bleyberg (Plombières,Belgique):Plomb, zinc mais aussi argent: Histoire, minéralisations, production d'argent, impact dans le paysage. *Geol. Surv. Belg.* **2011**, *310*, 57.

30. Rainbows, P.S. *Trace Metals in the Environment and Living Organisms: The British Isles as a Case Study*; Cambridge University Press: Cambridge, UK; New York, NY, USA, 2018; p. 741.

31. Heijlen, W.; Muchez, P.; Banks, D.A. Origin and evolution of high-salinity, Zn-Pb mineralizing fluids in the Variscides of Belgium. *Miner. Depos.* **2001**, *36*, 165–176.

32. Paradis, S.; Hannigan, P.; Dewing, K. Mississippi valley-type lead-zinc deposits. *Spec. Publ. Geol. Assoc. Can. Miner. Depos. Div.* **2007**, *5*, 185–204.

33. Dejonghe. L.; Boni., M. The "calamine-type zinc-lead deposits in Belgium and West Germany: a product of Mesozoic palaeo-weathering processes. *Geol. Belg.* **2005**, *8*, 3–14.

34. Muchez, P.; Heijlen, W.; Banks, D.; Blundell Boni, M.; Grandia, F. Extensional tectonics and the timing and formation of basin-hosted deposits in Europe. *Ore Geol. Rev.* **2005**, *27*, 241–267.

35. Jans, D.; Dejonghe, L. Les gisements plombo-zinciferes de l'est de la belgique. *Chron. Rech. Minière* **1983**, *470*, 3–24.

36. Coppola, V.; Boni, M.; Gilg, H.A.; Balassone, G.; Dejonghe, L. The "calamine" non-sulfide Zn–Pb deposits of Belgium: Petrographical, mineralogical and geochemical characterization. *Ore Geol. Rev.* **2008**, *33*, 187–210.

37. Abzalov, M.; Newman, C. Sampling of the mineralised tailings dumps ? case study of the Mount Morgan project, central Queensland, Australia. *Appl. Earth Sci.* **2017**, *126*, 1–5, doi:10.1080/03717453.2017.1343927.

38. Service Public de Wallonie, 2019, geoportail.wallonie.be/walonmap

39. Nikonow, W.; Rammlmair, D.; Furche, M. A multidisciplinary approach considering geochemical reorganization and internal structure of tailings impoundments for metal exploration. *Appl. Geochem.* **2019**, *104*, 51–59, doi:10.1016/j.apgeochem.2019.03.014.

40. Lam, E.J.; Carle, R.; González, R.; Montofré, Í, L.; Veloso, E.A.; Bernardo, A.; Álvarez, F.A. A Methodology Based on Magnetic Susceptibility to Characterize Copper Mine Tailings. *Minerals* **2020**, *10*, 939.

41. Loke, M.H. *Tutorial: 2-D and 3-D electrical imaging surveys. Course Notes for USGS Workshop 2-D and 3-D Inversion and Modeling of Surface and Drill hole Resistivity Data*; Course Notes for USGS Workshop, Torrs: CT, USA, 2004.

42. Dahlin, T.; Zhou, B. Multiple-gradient array measurements for multichannel 2D resistivity imaging. *Near Surf. Geophys.* **2005**, *4*, 113–123, doi:10.3997/1873-0604.2005037.

43. Günther, T.; Rücker, C.; Spitzer, K. Three-dimensional modelling and inversion of dc resistivity data incorporating topography - II. Inversion. *Geophys. J. Int.* **2006**, *166*, 506–517, doi:10.1111/j.1365-246x.2006.03011.x.

44. Caterina, D.; Beaujean, J.; Robert, T.; Nguyen, F. A comparison study of different image appraisal tools for electrical resistivity tomography. *Near Surf. Geophys.* **2013**, *11*, 639–658, doi:10.3997/1873-0604.2013022.

45. Oldenburg, D.W.; Li, Y. Estimating depth of investigation in dc resistivity and IP surveys. *Geophysics* **1999**, *64*, 403–416, doi:10.1190/1.1444545.

46. Baskaran, R.; Selvakumaran, T.; Subramanian, V. Aerosol test facility for fast reactor safety studies. *Indian J. Pure Appl. Phys.* **2004**, *42*, 873–878.

47. Goossens, D. Techniques to measure grain-size distributions of loamy sediments: a comparative study of ten instruments for wet analysis. *Sedimentology* **2007**, *55*, 65–96, doi:10.1111/j.1365-3091.2007.00893.x.

48. Mie, G. Beiträge zur Optik trüber Medien, speziell kolloidaler Metallösungen. *Ann. Phys.* **1908**, *330*, 377–445.

49. Shepard, F.P. Nomenclature Based on Sand-silt-clay Ratios. *J. Sediment. Res.* **2003**, *24*, 151–158, doi:10.1306/D4269774-2B26-11D7-8648000102C1865D.

50. Jackson, P.J.; Packham, R.F.; Richards, W.N. *The Examination of Organic flocculants and Coagulant Aids 8th Methods of Analysing Proprietary Chemicals Used in Water Supply Treatment Processes. Water Research Centre.* Technical Report TR6; Stevenage Laboratory: Stevenage, UK, 1975.

51. Frederickx, L. The Influence of Measurement Techniques on the Grain Size Distribution of the Boom Clay Formation. SCK-CEN I-0641, Mol, Belgium.

52.　El Ouahabi, M.; Chêne, G.; Strivay, D.; Auwera, J.V.; Hubert-Ferrari, A. Inter-technique comparison of PIXE and XRF for lake sediments. *J. Anal. At. Spectrom.* **2018**, *33*, 883–892, doi:10.1039/c8ja00019k.

53.　Bergmann, J.; Friedel, P.; Kleeberg, R. BGMN—A new fundamental parameter based Rietveld program for laboratory X-ray sources, its use in quantitative analysis and structure investigations. CPD Newsletter, Commission of Powder Diffraction. *Int. Union Crystallogr.* **1998**, *20*, 5–8.

54.　Lauwers, M. *Geotechnische Studie van een Mijn te Plombières*; Departement of Civil Engineering, Section Mining and Geophysical Engineering:, KU Leuven: Leuven, Belgium, **1992.**

55.　Santini, T.; Banning, N.C. Alkaline tailings as novel soil forming substrates: Reframing perspectives on mining and refining wastes. *Hydrometallurgy* **2016**, *164*, 38–47, doi:10.1016/j.hydromet.2016.04.011.

56.　García-Giménez, R.; Jiménez-Ballesta, R. Mine tailings influencing soil contamination by potentially toxic elements. *Environ. Earth Sci.* **2017**, *76*, 51, doi:10.1007/s12665-016-6376-9.

57.　Dominy, S.C.; Platten, I.M.; Raine, M.D. Grade and geological continuity in high-nugget effect gold–quartz reefs: implications for resource estimation and reporting. *Appl. Earth Sci.* **2003**, *112*, 239–259, doi:10.1179/037174503225003116.

58.　Jauniaux, M. Moresnet où l'histoire et la minéralogie se mêlent. *Lithorama* **2007**, 8, 10.

59.　Zhao, P.; Lu, L.; Liu, X.; De La Torre, A.G.; Cheng, X. Error Analysis and Correction for Quantitative Phase Analysis Based on Rietveld-Internal Standard Method: Whether the Minor Phases Can Be Ignored? *Crystals* **2018**, *8*, 110, doi:10.3390/cryst8030110.

60.　Jacobs, J.A.; Lehr, J.H.; Testa, S.M. *Acid Mine Drainage, Rock Drainage, and Acid Sulfate Soils: Causes, Assessment, Prediction, Prevention, and Remediation*; John Wiley & Sons, Inc.: Hoboken, NJ, USA, **2014**; p. 504.

61.　Leblanc, M.; Morales, J.A.; Borrego, J.; Elbaz-Poulichet, F. 4,500-year-old mining pollution in southwestern spain: Long-term implications for modern mining pollution. *Econ. Geol.* **2000**, *95*, 655–662, doi:10.2113/gsecongeo.95.3.655.

62.　Pascaud, G.; Leveque, T.; Soubrand, M.; Boussen, S.; Joussein, E.; Dumat, C. Environmental and health risk assessment of Pb, Zn, As and Sb in soccer field soils and sediments from mine tailings: solid speciation and bioaccessibility. *Environ. Sci. Pollut. Res.* **2014**, *21*, 4254–4264, doi:10.1007/s11356-013-2297-2.

63.　Moles, N.; Smyth, D.; Maher, C.; Beattie, E.; Kelly, M. Dispersion of cerussite-rich tailings and plant uptake of heavy metals at historical lead mines near Newtownards, Northern Ireland. *Appl. Earth Sci.* **2004**, *113*, 21–30, doi:10.1179/037174504225004439.

64.　Kicińska, A. Physical and chemical characteristics of slag produced during Pb refining and the environmental risk associated with the storage of slag. *Environ. Geochem. Health* **2020**, 1–19, doi:10.1007/s10653-020-00738-5.

65.　PERC. *Reporting Standard. Pan-European Standard for Reporting of Exploration Results, Mineral Resources and Reserves*; The Pan-European Reserves and Resources Reporting Committee: Brussels, Belgium. Available online:https://inspire.ec.europa.eu/co-delist/ClassificationAndQuantificationFrameworkValue/PERC (accessed on 16 February, 2017)

66.　Liu, Q.; Li, Y.; Zhao, G. The Latest Research Progress of Green Building Materials in Lead and Zinc Tailings. *IOP Conf. Ser. Earth Environ. Sci.* **2019**, *267*, 052024, doi:10.1088/1755-1315/267/5/052024.

67.　Kuranchie, F.A.; Shukla, S.K.; Habibi, D. Utilisation of iron ore mine tailings for the production of geopolymer bricks. *Int. J. Mining, Reclam. Environ.* **2014**, *30*, 92–114, doi:10.1080/17480930.2014.993834.

68.　Fontes, W.C.; De Carvalho, J.M.F.; Andrade, L.C.; Segadães, A.M.; Peixoto, R.A. Assessment of the use potential of iron ore tailings in the manufacture of ceramic tiles: From tailings-dams to "brown porcelain." *Constr. Build. Mater.* **2019**, *206*, 111–121, doi:10.1016/j.conbuildmat.2019.02.052.

69.　Achternbosch, M.; Bräutigam, K.-R.; Gleis, M.; Hartlieb, N.; Kupsch, C.; Richers, U.; Stemmermann, P. *Heavy Metals in Cement and Concrete Resulting from the Co-Incineration of Wastes in Cement Kilns with Regard to the Legitimacy of Waste Utilisation, FZKA 6923*; Forschungszentrum: Karlsruhe, Germany, **2003**; p. 200.

70.　*Belgium Legislave on Regulation on Sustainable Management of Material Cycles and Waste Materials (VLAREMA)*, Decree: Flanders, Belgium, p. 187. Available online: https://navigator.emis.vito.be/mijn-navigator?woId=44696 (accessed on 17 February, 2012**)**

71.　Dondi, Michele. (2003). Technological and compositional requirements of clay materials for ceramic tiles. Proc. 12th Int. Clay Conference, Bahía Blanca, Argentina, **2001.** doi:23-30. 10.1016/B978-044450945-1/50092-0.

72.　Dittmann, J.; Willenbacher, N. Microstructural investigations and mechanical properties of macroporous ceramic materials from capillary suspensions. *J. Am. Ceram. Soc.* **2014**, *97*, 3787–3792.

73.　Kambale, K.; Mahajan, A.; Butee, S.P. Effect of grain size on the properties of ceramics. *Met. Powder Rep.* **2019**, *74*, 130–136, doi:10.1016/j.mprp.2019.04.060.

74.　Veiga Simão, F.; Chambart, H.; Vandemeulebroeke, L.; Cappuyns, V. Sustainable use of sulfidic tailing residues in the production of ceramic roof tiles [Abstract]. In *Programme and Book of Abstracts of the 13th Conference for Young Scientists in Ceramics (CYSC-2019)*; Srdić, V.V., Ed.; Faculty of Technology, University of Novi Sad: Novi Sad, Serbia, **2019**; pp. 97–98.